DOI: 10.1002/ejic.201100539

Tailor-Made MgF_2-Based Catalysts by Sol–Gel Synthesis

Erhard Kemnitz,*[a] Stefan Wuttke,[a,b] and Simona M. Coman[c]

Keywords: Nanoparticles / Magnesium / Fluorides / Heterogeneous catalysis / Sol–gel processes

In this paper, recent developments in the field of catalysts based on nanosized metal fluorides are presented with special focus on the exciting and promising magnesium fluoride systems. The majority of these new catalyst systems originate from the work of the authors based on the fluorolytic sol–gel synthesis of metal fluorides, which was developed by this group. They are selected in a way as to highlight the principles and prospects of this new approach to high-surface-area, strongly distorted metal fluorides. This new fluorolytic sol–gel route to metal fluorides opens, in the opinion of the authors, a very broad range of scientific and technical applications of the accessible high-surface-area metal fluorides. By combining fluorolytic and hydrolytic sol–gel synthesis, this approach can be further extended, also providing access to metal hydroxide fluorides or metal oxide fluorides. The different synthesis strategies as well as the catalytic applications of various MgF_2-based materials are described in detail in this review.

1. Introduction

The preparation of catalysts is both art and science, but first of all, it is based on experience. Although the underlying chemistry is largely known, many industrial catalytic processes are so complicated that it is impossible to describe the scheme of chemical reactions involved in full detail. One of the very few famous exceptions is the synthesis of NH_3, which was investigated mechanistically for many years by Ertl and co-workers[1] because of its high relevance for society. As more than 80% of all the processes in chemistry are catalytic, the performance of the catalysts involved is crucial with regard to further improvements. Therefore, the current goal for material chemists is the development of novel and feasible approaches for high-performance heterogeneous catalysts. The second challenge for the development of new catalysts is to achieve 100% selectivity for the desired product molecule in order to follow the principles of "green chemistry".[2] The key to approaching these challenging goals lies in the synthesis of nanostructured materials. The ability of increasing the specific surface area by one order of magnitude by decreasing the particle size[3] is essential for materials that are involved in chemical reactions taking place on their surface. Moreover, nanostructured materials with high surface-to-volume ratio can display totally different properties as compared with macroscopic bulk materials. Therefore, materials with the same elemental constitution may exhibit totally different catalytic properties ranging from not being active at all to being 100% active and, in the best case, being 100% selective for the desired product as well.

Especially in the case of metal oxides, but also in the case of noble metals, nanomaterials have been proven to exhibit such exciting catalytic properties. In the case of metal fluorides, synthesis approaches toward nanoscopic metal fluorides have been developed just in the very recent years, and they have given similar access to new catalytic materials. Our recent studies have demonstrated that the *fluorolytic* sol–gel process can be used as a powerful bottom-up approach for the synthesis of highly catalytically active and selective metal fluorides.[4,5] Having sol–gel chemistry in mind, one almost implies the reaction of water with metal alkoxides in a suitable solvent that results in the formation of new materials, but based on metal oxide phases [Equation (1)].

$$M(OR)_n + nH_2O \rightarrow M(OH)_n + nROH \quad (1)$$

In fact this *hydrolytic* sol–gel process is based on network formation by means of hydrolysis followed by condensation reactions of metal alkoxy and metal hydroxy groups, resulting "per definition" in the formation of M–O–M bonds, and thus, under appropriate conditions, in the formation of a stabilized sol that contains nanometal oxide particles.[6,7] With time, the nanoparticles link together to become a three-dimensional gel network. Removal of the solvent followed by a calcination procedure results in porous materials with high surface area (schematically shown in Figure 1). Although this explanation is a drastic simplification of the chemistry going on, this approach has become one of the most versatile and powerful synthesis routes to nanoscopic materials.

[a] Department of Chemistry, Humboldt-Universität zu Berlin, Brook-Taylor-Strasse 2, 12489, Berlin, Germany
Fax: +49-30-20937468
E-mail: erhard.kemnitz@chemie.hu-berlin.de
[b] Department of Chemistry and Center for NanoScience (CeNS), University of Munich (LMU), Butenandtstraße 11, 81377 München, Germany
[c] Department of Chemical Technology and Catalysis, Faculty of Chemistry, University of Bucharest, Bdul Regina Elisabeta 4-12, 030016 Bucharest, Romania

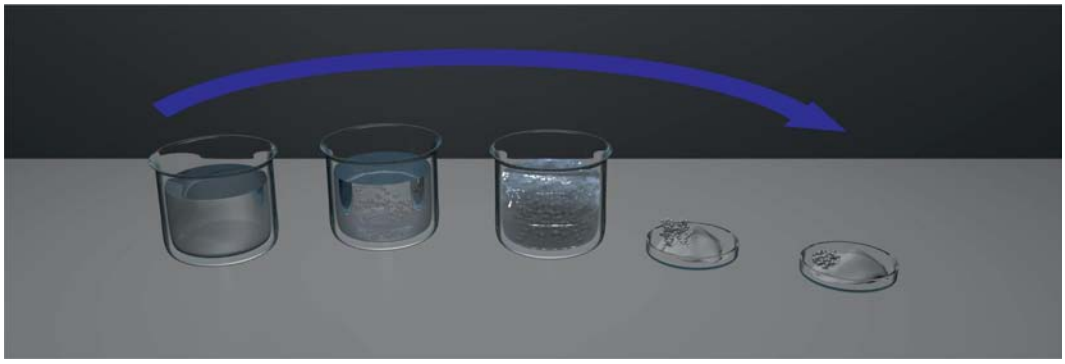

Figure 1. Graphical illustration of the different steps of the sol–gel process. Step 1: molecular precursor (typically metal alkoxides); step 2: formation of a transparent sol that consists of nanoparticles with diameters of 1–100 nm; step 3: cross-linking of the nanoparticles to a three-dimensional network; step 4: removal of the solvent; step 5: post-treatment of the material.

However, since 2003[8] sol–gel chemistry was extended by the so-called *fluorolytic* sol–gel route. The principle of this soft chemistry approach is based on the reaction of a metal alkoxide with anhydrous HF (instead of H_2O) in alcohol solution, resulting in an exchange of OR by F [Equation (2)]. *CAUTION: HF is a highly toxic and irritant compound causing severe burns if it comes in contact with the skin!*

$$M(OR)_n + n\text{HF} \rightarrow MF_n + n\text{ROH} \quad (2)$$

This method has been successfully employed for the synthesis of nanoscopic, high-surface-area (HS) aluminium fluoride (HS-AlF_3) and was then successfully applied for the synthesis of several other nanometal fluoride systems.[4] However, *fluorolytic* sol–gel synthesis is not only limited to metal fluorides but can be modified in a way to make further functionalization possible [Equation (3)].

$$M(OR)_n + (n - m)\text{HF} + m\text{HOX} \rightarrow MF_{n-m}(OX)_m \quad (3)$$

If group X is H (the reactant molecule is water, which competes with HF), hydroxide fluorides might be accessible. If X is, for example, any carboxylic substituent, organically functionalized nanoscopic metal fluorides might be available. Thus, the *fluorolytic* sol–gel route opens in principle all the synthesis routes that are known for the respective metal oxide systems. However, in case of related systems prepared by the sol–gel route, many thousands of research groups have worked over the past thirty to forty years, in case of nanoscopic metal fluorides obtained by the *fluorolytic* sol–gel approach, research in the field has just started. Nevertheless, some notable and promising approaches have already been achieved, showing that this synthesis route opens a very broad range of technical applications as well as giving access to fundamental research.[4,5]

Erhard Kemnitz, born in 1951, studied chemistry at the Humboldt-Universität zu Berlin (Germany) and obtained his diploma degree in 1973. In 1977 he completed his doctoral degree at the same university under the supervision of Dieter Hass with a thesis on the kinetics and mechanism of solid–gas reactions. He received a Humboldt award for this thesis in 1978. After working as a lecturer for Chemical Engineers for one year, he returned to the Humboldt-Universität and finished his Habilitation in 1986 on heterogeneous chlorine/fluorine exchange reactions. In 1988 he became an assistant professor and in 1994 he received a full-time tenure track, both at the Humboldt-Universität zu Berlin. He was head of the Chemistry Department of Humboldt University from 2001 to 2004. He is member of the editorial board of the Journal of Fluorine Chemistry. His main research interests cover the synthesis and characterization of strongly distorted nanoscopic metal fluorides for applications in the field of heterogeneous catalysis, optics, ceramics, surface coating and so on. He published about 350 papers, 8 review articles, 8 books and/or book chapters, and filed 6 patents. In 2010 he founded "nanofluor GmbH".

Stefan Wuttke was born in 1980 in Guben (Germany) and completed his Diploma in chemistry in 2005 at the Humboldt Universität zu Berlin in cooperation with the University of Glasgow. He completed his PhD in 2009 with Prof. E. Kemnitz at the Humboldt-Universität zu Berlin. For his postdoctoral research he moved to the Institute Lavoisier de Versailles (Prof. G. Férey) and Laboratoire Catalyse et Spectrochimie – ENSICAEN (Prof. M. Daturi), supported by a Feodor Lynen grant. Since 2011 he is working in the group of Prof. T. Bein at the Universität München (LMU) as junior researcher pursuing a habilitation, supported by a Return Fellowship from the Alexander-von-Humboldt Foundation. His research concerns synthesis, characterization and application of porous materials, particularly structure–reactivity as well as host–guest relationships in metal fluorides and MOFs.

Simona M. Coman received her diploma as a Chemist from the University of Bucharest in 1992. Since then, she has worked in the group of Prof. V. I. Parvulescu in the Department of Chemical Technology and Catalysis. Her PhD dissertation on "Enantio- and Diastereoselective Catalytic Hydrogenations" was published in 2001 under the guidance of Prof. Em. Angelescu. In 2007 she worked as a research fellow of the Alexander-von-Humboldt Foundation in the group of Prof. E. Kemnitz in the Institut für Chemie, Humboldt-Universität zu Berlin. In 2008 she became Professor in the Department of Organic Chemistry, Biochemistry and Catalysis, University of Bucharest. Her areas of interest include the synthesis of heterogeneous catalysts and catalytic processes, such as those of chemo-, enantio- and diastereoselective hydrogenation, isomerization, acylation, as well as the catalytic synthesis of fine chemical and pharmaceutical intermediates.

Especially nanoscopic magnesium fluoride prepared in this way is suitable for several applications like antireflective coatings and ceramics, as well as showing unexpected new catalytic properties.

Therefore, in this review we will highlight recent results on the synthesis and catalytic applications of MgF_2-based materials prepared by the *fluorolytic* and the mixed *fluorolytic/hydrolytic* sol–gel synthesis. For this purpose, we summarize at first the state of the art of the magnesium fluoride system in general, showing that this research field has significantly expanded in the last years. Afterwards, the *fluorolytic* sol–gel process is described with respect to the synthesis of MgF_2-based materials.

One of the most exciting aspects in this regard arises from the synthesis route according to Equation (3) with water as competing co-reactant. For the first time, magnesium hydroxide fluoride phases can be prepared, which exhibit unique catalytic properties as will be outlined later. The Lewis and Brønsted properties of these materials can be tuned over a wide range by monitoring the ratio of F to OH in the $MgF_{2-x}(OH)_x$ phases, which results in a wide variety of acid–base surface sites. As a matter of fact, this can easily be done by changing the amount of H_2O and/or HF added to the magnesium alkoxide solution. Finally, by a simple postcalcination treatment, not only is the removal of traces of the organic solvent possible but also dehydroxylation (350 °C), which transforms the nanometal hydroxide fluorides into the respective oxide fluorides. In this way, these new catalysts can be prepared by a process that is cheap and easy to scale up, which might also become interesting for industrial applications. It is worth mentioning that the reaction of the metal alkoxide solution with HF can be performed in glass containers, as when the organic HF solution (only this has to be stored in plastic vessels) is added, the HF immediately becomes "neutralized", meaning free HF is no longer present in the reaction system. The company *nanofluor GmbH* (www.nanofluor.de) has started to commercialize these new materials based on our own patents and offers such nanometal fluorides obtained by the fluorolytic sol–gel route.

This review is intended to underline the link between the chemical knowledge of the acid–base properties of the catalyst surface and the demand arising from the chemical reaction involved. Moreover, we would like to provide evidence of trends aimed at improving the process by selective changes of the acid–base properties of the catalytic material. For this purpose we present here the fluorolytic as well as the combined fluorolytic/hydrolytic sol–gel synthesis of different MgF_2-based materials as a platform for easily tuneable acid–base catalysts.

2. State of the Art of MgF_2

Over the past years, magnesium fluoride has attracted increasing interest due to its unique optical properties combined with its high chemical and mechanical durability. The actual research fields involving MgF_2 are summarized in Scheme 1.

Scheme 1. Summary of the actual research fields involving MgF_2.

MgF_2 is a white salt that crystallizes in a rutile-type structure (*tP*6), space group $P4_2/mmm$ No. 136.[9,10] Two different views of the rutile structure of MgF_2 are shown in Figure 2.

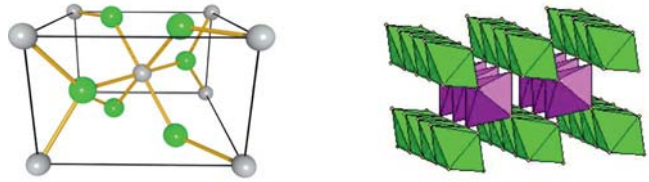

Figure 2. Sketch of the rutile structure of MgF_2 (left) and the octahedral arrangement in the 3D structure (right). The 3D structure can be rationalized by chains of edge-bridged MgF_6 octahedra that are corner-bridged to an adjacent chain.

In crystalline, tetragonal MgF_2 (ICSD 56506, PDF No. 41–1443), the Mg atom is octahedrally coordinated by six F atoms (Niggli notation: $MgF_{6/3}$) and has one crystallographically unique fluorine atom, which coordinates three Mg atoms (M–F bond lengths: 2.0119, 2.0119 and 1.9883 Å; Mg–F–Mg bond angles: 129.9, 129.9 and 100.2°).

Jansen and co-workers explored the energy landscape (i.e., all possible spatial arrangements of all atoms) of many crystalline structures by performing intense theoretical calculations.[11] For the energy landscape of MgF_2, they found two energy minima: one with a rutile and the other with an anatase structure.[12,13] However, the anatase-type structure is not easily available in real experiments or during the optimization runs, because its minimum is surrounded by rather high energy barriers essentially prohibiting access at temperatures below the trapping temperatures of the competing rutile local minima.[14] Thus, until now all experimental data provide evidence for the existence of MgF_2 in the rutile structure only.

More relevant for this review is that Jansen and coworkers extended their concept of energy landscape for not-yet-synthesized compounds and studied the landscape of some magnesium oxide fluoride compositions.[15] This analysis showed that magnesium oxide fluoride compositions are stable and can exist without phase separation into the very stable binary phases MgO and MgF_2. This prediction is in full agreement with the current state of the art that was achieved by our group very recently based on the

new *fluorolytic* sol–gel approach, which will be discussed in greater detail in this review.

The pyrohydrolysis and hydrolysis stability of a metal fluoride is an important issue, because fluorides may react with water with elimination of HF. It was found that, among a huge batch of fluorides, MgF_2 is one of the most stable with respect to pyrohydrolysis (tested at 1000 °C)[16] as well as hydrolysis.[17] The solubility of MgF_2 is 0.0002 g per 100 g H_2O at room temperature, and exposure to 100% relative humidity at room temperature does not fog polished MgF_2 surfaces even after one month.[18]

Magnesium fluoride is transparent over an extremely wide range of wavelengths ranging from 0.11 to beyond 7.5 microns depending on the thickness of the window.[19] Along with LiF, MgF_2 is one of the two materials that transmit in the vacuum ultraviolet range. Moreover, it is also used to some extent for the infrared transmission range but with limitation because it is expensive in comparison to CaF_2. Recently, Nofar and co-workers characterized the dependency of the optical properties of hot pressed MgF_2 on its density.[20] They could demonstrate that eliminating the pores and increasing the relative density are the main factors that affect transparency. With respect to this result, a second study followed, reporting the preparation of dense polycrystalline MgF_2 ceramics by using MgF_2 powders of two different sizes.[21] The first powder was synthesized by a precipitation method with NaF and $MgCl_2$, and the second powder was commercial microsized MgF_2 that was treated by milling. It was shown that the sample with 15 wt.-% of the first powder has the best transparency due to a maximal elimination of the pores and a maximal relative density of the sample.

The second important commercial application of MgF_2 is its use as material for thin layers for protective and antireflective coatings produced by sputtering or chemical vapour deposition CVD.[22–24] Despite all the advantages of MgF_2 (chemical stability and high transparency) mentioned above, its low refractive index (n_{500} = 1.38) is evidently the outstanding key feature for antireflective (AR) and low-refractive-index materials. Therefore, new approaches for MgF_2 thin films were proposed in the last years with the aim to overcome the complex and corrosive gas phase deposition methods to avoid corrosive gases such as HF and F_2. The major disadvantage of gas-phase deposition methods, however, is the fact that it leads to nonstoichiometric MgF_2 layers (F-centre formation), making the technical application difficult.

Consequently, Fujihara et al. introduced the preparation of MgF_2 films from the liquid phase by a trifluoroacetic acid (TFA) method.[25,26] Magnesium ethoxide was treated with TFA, which resulted in the formation of magnesium trifluoroactetate sols that can be used for the formation of thin films by spin coating. MgF_2 thin films were obtained by heat treatment of these films at 300 °C in air. Unfortunately, the formation of impurities (MgO) was observed, and therefore industrial application of this method is limited.

A sol of nanocrystalline MgF_2 was synthesized by A. A. Rywak and J. M. Burlitch by the reaction of hydrofluoric acid on a sol prepared from H_2O_2 and $Mg(OCH_3)_2$ in methanol solution.[27] Thin films spin coated on Si(100) also showed the formation of MgO after being calcined in dry air, and hence the optical properties were less suitable in comparison with pure MgF_2.

A pure thin film of MgF_2 with high-quality optical properties could be realized by using MgF_2 sols obtained by the *fluorolytic* sol–gel synthesis (described in detail below).[28] The MgF_2 sol was prepared from a suspension of $Mg(OCH_3)_2$ in methanol and a nonaqueous HF solution in methanol. From these sols, MgF_2 can be deposited on silicon or glass substrates by using spin- or dip-coating techniques. Furthermore, this method allows the preparation of thin films with defined thickness for use in optical AR layers. Moreover, MgF_2 and TiO_2 homogeneous layer stacks were produced by a spin-coating sol–gel process.[29] In other words, it was shown that it is possible to produce layer stacks consisting of a low-refractive-index metal fluoride (MgF_2; n_{500} = 1.38) and a high-refractive-index metal oxide (TiO_2; n_{500} = 2.1) by a sol process. The further extension of this approach to any other metal fluoride and metal oxide is currently under investigation.

Recently, the group of Sanchez reported the preparation of magnesium oxide fluoride vesicle-like porous coatings with extremely low refractive indices down to 1.09 (the lowest reported refractive index is 1.08).[30,31] The precursor solution is composed of magnesium acetate, trifluoroacetic acid (TFA) as fluorine source, ethanol and water. The thermal treatment (ramp rate) and the calcination atmosphere (water content) are critical parameters for the dip-coating substrates. Furthermore, Fujihara demonstrated that with a similar TFA approach different kinds of oxide fluoride materials with optical functions can be obtained.[32] This work demonstrates nicely how things can be improved (in this case optical properties) by combining fluoride and oxide materials.

The properties and prospects of application of fluoride nanoparticles were recently reviewed by Kuznetsov et al.[33] The different approaches developed in the last years to control the particle size and morphology of MgF_2 were investigated. The following summary will give a rough survey of recent work in the field of nanofluorides without considering the *fluorolytic* sol–gel synthesis of nanoscopic MgF_2, which will be described in more detail in the next sections of this review.

Porada and co-workers reported the synthesis of MgF_2 powder with crystallite size in the range 9–11 nm and a specific surface area of 190 $m^2 g^{-1}$.[34] This was achieved by precipitation in microemulsions of water in cyclohexane stabilized by polyethylene glycol *tert*-octylphenyl ether. Unfortunately the authors were not able to remove all organic residues, which limits the application of the material obtained. The group of Skapin used an oxidative decomposition approach (with F_2 gas in liquid HF) resulting in a partially crystallized MgF_2 with a surface area of 70 $m^2 g^{-1}$.[35] Hu and co-workers synthesized MgF_2 nanorods with diameters between 60 and 100 nm by a microemulsion method.[36] The group of Wojciechowska used a microwave-assisted synthe-

sis for spherical monodisperse MgF_2 particles with rather large diameters of 0.25 μm but with high monodispersity.[37] Sekonkaev et al. reported a precipitation method by using NaF as the fluoride source and $MgCl_2$.[38,39] By changing experimental parameters, such as the pH, MgF_2 was prepared as uniform crystals of different appearance (ranging in size from 50 to 100 nm) or as polycrystalline spheres. The authors point out the problem of complexity related to the preparation of uniform particles of a given chemical composition and shape by the precipitation process. The best approach for a controllable size of magnesium fluoride particles was reported by Okuyama and co-workers.[40] By changing the molar ratio of $NH_4F/MgCl_2$, particles of size ranging from 6 to 300 nm with spherical and cubic morphology could be prepared. It is obvious that these investigations are in their infancy and will be further developed, in particular, with use of the nanoparticle solution for the preparation of thin films.

The use of MgF_2 as a support for catalytically active phases was first reported by Wojciechowska[41] and already reviewed in 2003.[42] The idea is to use a chemically inert surface as support that, in addition, does not contain any oxide ions and might be distinguishable from metal oxide catalysts. Recent work used MgF_2 as a support material for the preparation of active catalysts for CO oxidation,[43] NO decomposition and reduction by C_3H_6[44] and selective reduction of chloronitrobenzene to chloroaniline on Ru/MgF_2 catalyst.[45] Additionally Martin and co-workers reported the evaluation of V_2O_5 catalysts supported on MgF_2 for ammoxidation of 3-picoline.[46,47]

At this point it is important to note that the different fields of MgF_2 applications, as summarized in Scheme 1, have attracted increasing interest from different research groups especially in the past five years. The authors are convinced that this is just the beginning of a further acceleration of the application of nanoscopic metal fluorides, especially of MgF_2. Since the application of MgF_2 in antireflective coating processes has already achieved a fundamental attraction, it is the opinion of the authors that magnesium fluoride and magnesium hydroxide fluorides will have a similar impact on catalytic applications. Therefore, this paper will review recent achievements resulting from the availability of these new materials.

3. Sol–Gel Synthesis of MgF_2-Based Materials

Various MgF_2-based nanoscopic materials can be successfully produced by the *fluorolytic* sol–gel technique. This sol–gel process is a simple, soft-chemical synthesis that is based on the room-temperature reaction of magnesium alkoxide with HF. Magnesium methoxide was used as precursor, because it can be synthesized easily by the reaction of magnesium with dry methanol. Moreover, investigation of the influence of different magnesium alkoxides for the final properties of MgF_2 revealed that the surface properties remained unchanged.[48] The overall reaction [Equation (4)] of dissolved HF in methanol with a methanol solution of $Mg(OCH_3)_2$ leads to the nearly quantitative formation of the fluorinated product.

$$Mg(OCH_3)_2 + xHF \rightarrow MgF_x(OCH_3)_{2-x} + xROH \quad (4)$$

Although a stoichiometric amount of HF is used and the nucleophilic substitution reaction is thermodynamically favoured, the reaction is kinetically controlled because of the viscosity of the gel. However, this does not hold for very diluted systems of low viscosity such as those used for the preparation of MgF_2 thin films.[28] On the other hand, a completely fluorinated MgF_2 is also not required for the synthesis of a bifunctional catalyst. Moreover, the bulk composition of the magnesium methoxide fluoride already almost corresponds to MgF_2.[48] Traces of methanol and methoxide still present mainly at the surface can be removed with a gentle post-treatment in order to get a clean and active surface.

Although the reaction of a stoichiometric amount HF with $Mg(OCH_3)_2$ yields nearly X-ray-amorphous material,[48] the reaction [Equation (4)] was used for the synthesis of the first single-crystal structure of an alkoxide fluoride alkaline earth metal compound.[49] The partial fluorolysis of magnesium methoxide (reaction mixture with an F/Mg ratio ranging from 0.2 to 0.5) transforms the cubane structure units of crystalline magnesium methoxide into hexanuclear dicubane units containing μ_4-fluorine atoms. The resulting $[Mg_6(\mu_4\text{-}F)_2(\mu_3\text{-}OMe)_4(MeOH)_{12}][H(MeO)_2]_2$ compound crystallizes in two different modifications and is to date the only stable crystalline intermediate magnesium methoxide fluoride that could be isolated (Figure 3).[50]

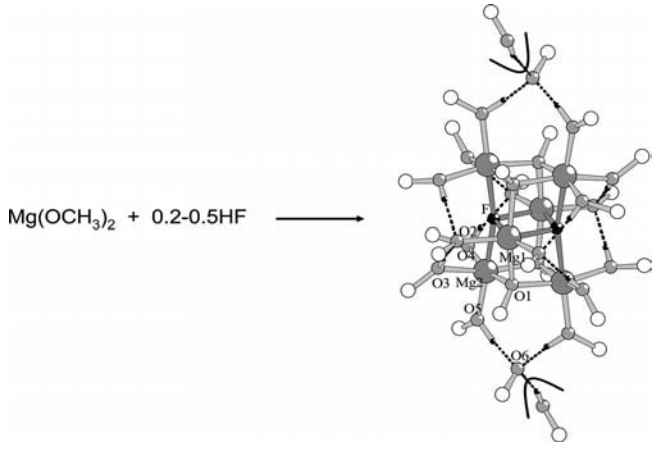

Figure 3. The structure of $[Mg_6(\mu_4\text{-}F)_2(\mu_3\text{-}OMe)_4(MeOH)_{12}]$-$[H(MeO)_2]_2$ with a hexanuclear dication and two anionic MeO···HOMe units connected to the cation and structure after losing the solvated methanol indicated by two solid separating lines.[50] Reproduced by permission of the Royal Society of Chemistry.

However, all MgF_2-based materials that will be described below are either nanocrystalline or amorphous. The *fluorolytic* sol–gel reaction [Equation (4)] results in the formation of monodisperse MgF_2 particles with an average diameter between 3 and 5 nm. For the synthesis of materials, the solvent phase must be removed; this can easily be achieved under vacuum. During this drying process, a gel

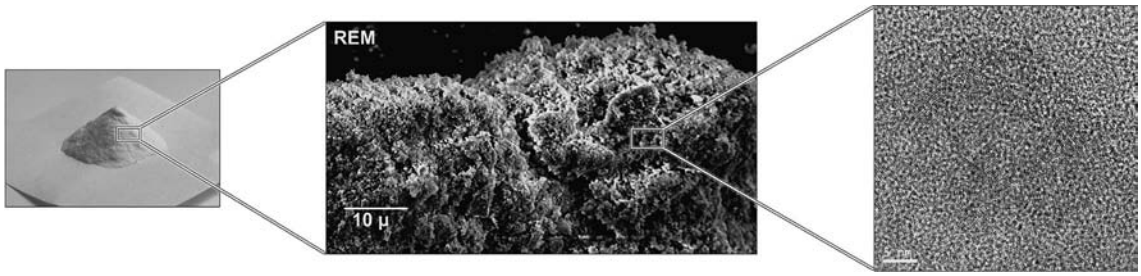

Figure 4. Picture of $MgF_{2-x}(OH)_x$ powder; SEM image of a $MgF_{2-x}(OH)_x$ particle, HRTEM image of a $MgF_{2-x}(OH)_x$ cluster on a carbon support film.

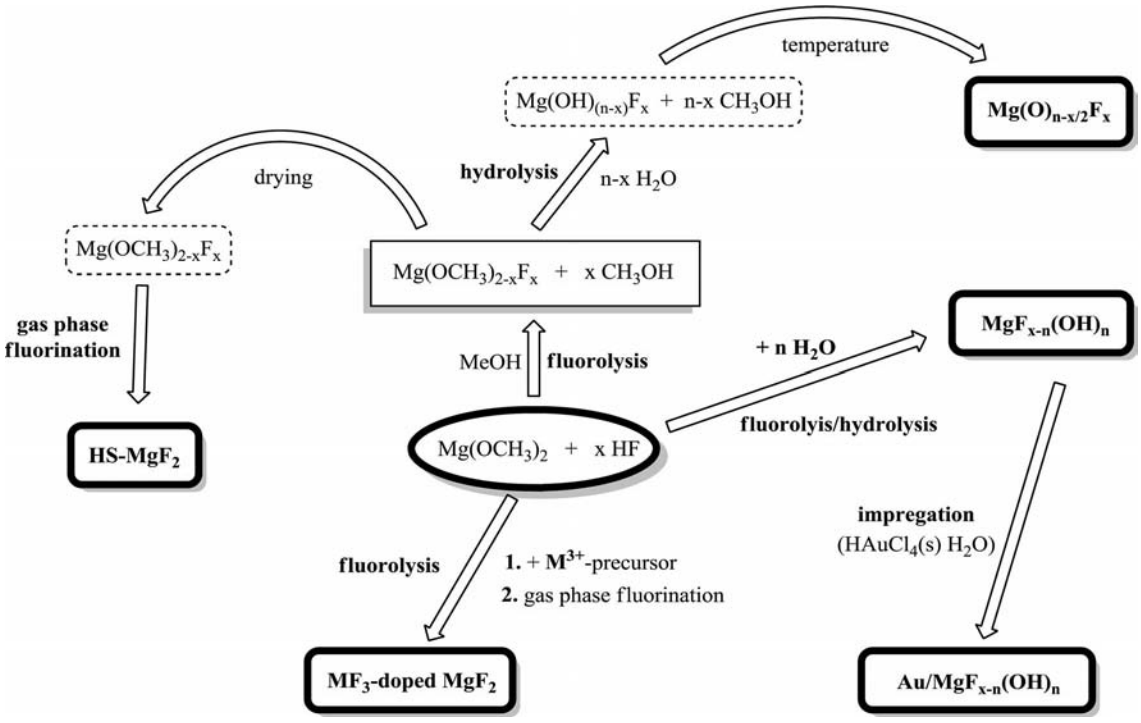

Figure 5. Schematic representation of the different reaction approaches all based on the *fluorolytic* sol–gel synthesis.

is formed that contains a three-dimensional network of the nanoparticles (Figure 1). This gel network persists for our cases in the bulk material and forms nanoscopic materials with high porosity (Figure 4). Both properties – high porosity, which means high surface area, as well as nanoscopic size, which means agglomerated nanoparticles – are the key for a high number of active sites, which are essential for a good catalyst.

This section focuses on the synthesis strategies and characterization of different MgF_2-based compounds. As demonstrated in Figure 5, the *fluorolytic* sol–gel reaction [Equation (4)] can be used as a platform for the synthesis of different tuneable acid–base as well as bifunctional catalysts.

3.1. Sol–Gel Synthesis of Magnesium Fluoride

The synthesis of MgF_2 consists of a two-step process: (1) reaction of the magnesium methoxide with a stoichiometric amount of nonaqueous HF solution in methanol; (2) the gas-phase fluorination of the obtained dry gel (Figure 5).[48,51] This postfluorination can be done with HF at 120 °C in order to form a nearly X-ray-amorphous, high-surface-area magnesium fluoride, which is named HS-MgF_2. The nitrogen adsorption–desorption data at 77 K indicates that the sample is mesoporous with a BET surface area of 200 to 250 $m^2 g^{-1}$.[48] Unfortunately, this compound is not very stable: at around 200 °C crystallization starts, and with this the surface area decreases. MgF_2 synthesis by gas-phase fluorination with $CHClF_2$ at 350 °C produces a lower-surface-area material, which nevertheless has very interesting surface properties. The acidity and basicity of this compound was extensively characterized by FTIR spectroscopy with adsorbed probe molecules.[52] The probe molecules interact with the surface sites of the material, and the alteration of the spectral features as a result of adsorption provides information about the acid–base centres on the surface of the investigated material.[53]

By applying the existing knowledge on undercoordinated magnesium sites on the surface of magnesium oxide,[54] all CO bands on magnesium fluoride could be assigned. MgF_2

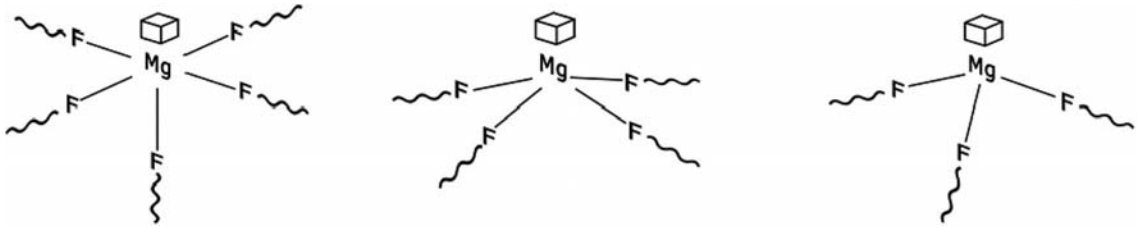

Figure 6. Three-, four-, and fivefold-coordinated magnesium atom sites in MgF_2 prepared by the sol–gel method.

prepared by the sol–gel method displays five-, four- and threefold-coordinated surface magnesium sites, as shown in Figure 6. The strength of these Lewis acid sites depends on the coordination of the metal cation: the lower the coordination the stronger the acidity, and hence, the higher the ν(CO) frequency (Table 1). Moreover, at high CO pressures dicarbonyl species are formed on fourfold-coordinated magnesium. The strength of the Lewis acid sites ranges from moderate (three- and fourfold-coordinated magnesium) to weak (fivefold-coordinated magnesium), but their number is very high (5–6 sites nm^{-2}). This high number of sites is a result of the nanoscopic nature of the material (Figure 4), and it must be noted that the real number is actually even higher, because it is not possible to detect all fivefold-coordinated magnesium sites, as the investigation must be carried out at very low temperature ($T < 60$ K).[54]

Table 1. Observed wavenumbers (in cm^{-1}) of CO adsorbed on MgF_2 prepared by the sol–gel method and assignment of the ν(CO) bands.[52]

Mg^{2+} coordination	ν(CO) band	Carbonyl species
Threefold	2201–2189	Monocarbonyl species
Fourfold	2187–2181	Monocarbonyl species
Fourfold	2186, 2176	Dicarbonyl species
Fivefold	2168	Monocarbonyl species

In addition to the acidity of MgF_2, we explored for the first time the basicity of fluorine atoms on the surface of a metal fluoride.[52] Pyrrole clearly showed the presence of basic sites on the MgF_2 surface, which are characterized by two bands [ν(N–H) = 3415 and 3270 cm^{-1}]. The ν(N–H) band in pyrrole N···X complexes can be related to the strength of this interaction,[55] and indicates for sol–gel prepared MgF_2 one weakly and one moderately basic site. Aside from these species, the formation of a π complex was observed between Mg^{2+} Lewis acid sites and the aromatic ring. Moreover, the adsorption of $CHCl_3$ revealed the dominating presence of Lewis acid sites at the MgF_2 surface. $CHCl_3$ is used as a probe molecule for the characterization of acid–base pairs, and it can interact separately with either a Lewis base site or an acid site but simultaneously with both sites as well.[56,57] The adsorption of $CHCl_3$ mainly occurs at Lewis acid sites and to some extent simultaneously at Lewis acid and base sites.[52] It can be concluded from all these results that MgF_2 prepared by the sol–gel method presents a high number of moderately strongly Lewis acidic sites and some weakly basic sites. With this knowledge it was possible to explain all bands arising from Lewis acid–base pairs by the adsorption of water, which is coordinated to Lewis acid sites and at the same time hydrogen-bonded to fluorine atoms. Therefore, such interaction might also occur during the catalytic process, and this knowledge will be helpful for understanding the catalytic behaviour. Moreover, the large number of sites explains the unique catalytic properties[58] of the surface of MgF_2 prepared by the sol–gel method in comparison with the inert surface of conventionally prepared MgF_2.[42]

3.2. Sol–Gel Synthesis of MF_3-Doped Magnesium Fluorides

Nanoscopic MgF_2 prepared by the sol–gel method exhibits moderately strong Lewis acidity due to undercoordinated Mg^{2+} sites on the surface, which might be too weak for some organic reactions. On the other hand, if the Lewis acidity, for example in HS-AlF_3, is too strong, this results in the formation of byproducts and hence is not very selective and not suitable for the production of fine chemicals.[4] To overcome this problem, MF_3-doped magnesium fluorides were synthesized. The enhancement of Lewis acidity by aliovalent cation doping is known for oxides and was explored by Tanabe[59] and extended by Kemnitz et al. for fluorides.[60] The model is based on two assumptions: (1) The coordination number of the host as well as of the guest metal fluoride is maintained even when they form solid solutions. (2) The coordination number of the fluoride of the host component is retained for all fluorides.[60] By applying this model, for example to CrF_3-doped MgF_2, the generation of Lewis acidity is predicted. The realization of such a system is straight forward for *fluorolytic* sol–gel synthesis. A suitable M^{3+} precursor is added to the magnesium methoxide solution followed by the addition of HF and postfluorination (Figure 5). MF_3-doped MgF_2 materials prepared in this way reveal the validity of the hypothesis for this system. By using different guest metals (Cr, Fe, V, In, Ga), materials with different enhanced Lewis acidity were reported.[61–63] Hence, with nanoscopic pure magnesium fluoride prepared by the sol–gel method and ternary metal fluoride systems, materials with different strengths of Lewis acidity are accessible and could be applied for catalysis, as will be shown below.

3.3. Sol–Gel Synthesis of Magnesium Oxide Fluorides

The analogy of the *hydrolytic* and *fluorolytic* sol–gel process motivated us to combine the two synthesis routes. Both

approaches have a common starting point, a suitable metal alkoxide that undergoes a reaction either with water (hydrolysis) or with anhydrous hydrogen fluoride (fluorolysis). Thus, we explored the possibility to combine the two reaction routes by employing less than stoichiometric amounts of anhydrous HF in the first reaction step followed by the addition of the stoichiometrically required amount of water. This general process has already been successfully applied for the synthesis of magnesium oxide fluoride catalysts (Figure 5).[64] The exciting part of this approach is the possibility of varying the oxygen-to-fluorine ratios of the materials. It is important to consider this feature, because it strongly influences the acid–base properties of the surface and would eventually result in the possibility to tune them. Indeed, such materials must cover the range from strong Lewis base (pure magnesium oxide) to moderately strong Lewis acid (pure magnesium fluoride).

First of all an investigation of the bulk material was performed; it revealed the presence of magnesium oxide fluorides.[64] It was shown that the composition of the $MgF_{6-x}O_x$ octahedral units changes with the fluorine-to-oxygen ratio. Hence, magnesium oxide fluorides were obtained with high fluorine content built up from fluorine-rich and oxygen-poor $MgF_{6-x}O_x$ octahedra. As predicted by computer simulation,[15] these phases are quite stable and phase separation into the stable binary phases MgO and MgF_2 starts at around 500 °C. Moreover, these materials exhibit very large surface areas ranging from 300 to 500 $m^2 g^{-1}$. Interestingly enough, the acid–base properties of magnesium oxide fluorides depend on those of the reactants, and hence they can be tuned by monitoring the acid–base properties of pure MgO to pure MgF_2.[65] CO adsorption on different magnesium oxide fluorides showed a more pronounced blueshift in samples with higher fluorine content in comparison with that observed in samples with lower fluorine content. The strength of a Lewis acid site depends on the coordination of the metal cation and also on the ability of the ligands to withdraw electrons. All these samples exhibit five- and fourfold-coordinated magnesium surface sites,[65] which means that the different acid–base properties are not a result of differently coordinated Mg surface sites but are caused by the different chemical composition of these phases. The Lewis acidity of the undercoordinated magnesium atoms changes because fluorine is more electronegative than oxygen (Figure 7). Hence, magnesium oxide fluorides with high fluorine content contain more atoms with higher electronegativity than magnesium oxide fluorides with high oxygen content, and therefore the former are stronger Lewis acids. For the same reason, the Lewis basicity increases with decreasing fluorine but increasing oxygen content. CO_2 adsorption measurements prove this trend clearly and display a higher concentration of basic sites with higher oxygen content.[65] Therefore, chemical surface transformations induce changes in the acid–base properties of the material. This can be done in an easy and straightforward way by simply changing the HF to H_2O ratio in the synthesis protocol: by increasing the fluorine content of the magnesium oxide fluoride, the Lewis acidity is increased and the basicity is decreased. Therefore, the combination of the *hydrolytic* and *fluorolytic* sol–gel processes represents a powerful synthesis tool for obtaining high-surface-area materials with acid–base sites that can be tuned over a wide range.

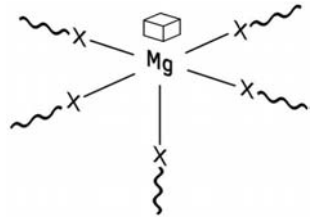

Figure 7. Accessible Lewis acid site on a magnesium fluoride surface (X = O, F).

3.4. Sol–Gel Synthesis of Partly Hydroxylated Magnesium Fluorides

Recently, we discovered the unexpected catalytic performance of nanoscopic hydroxylated magnesium fluoride, which was prepared by the combination of the *fluorolytic* and *hydrolytic* sol–gel processes.[66] In this synthesis, the stoichiometry of $M(OR)_x$ to xHF remains constant, but the water content is varied, and the hydrolysis becomes increasingly competitive with an increasing amount of water (Figure 5). The selective solvolysis of the original M–OR bond by aqueous HF results preferably in the formation of M–F but to a minor extent M–OH bonds. We successfully applied this general approach for a *one-pot* sol–gel synthesis of various partially hydroxylated magnesium fluorides.[66]

The $MgF_{2-x}(OH)_x$ samples prepared this way display the bulk structure of MgF_2 with no carbon content. Therefore, this indicates a complete solvolysis process where no post-treatment is necessary. When the amount of water is increased by using aqueous HF with concentrations from 100 wt.-% to 40 wt.-%, analyses by ^{19}F MAS NMR spectroscopy, TEM and XPS show an increase in the number of hydroxy groups mainly on the surface, whereas the bulk composition remains unchanged for all samples. This suggests the presence of shell-like nanoparticles of $MgF_{2-x}(OH)_x$ phases, where the inner cores (bulk) mainly consist of pure MgF_2 and the outer shell (surface) becomes increasingly hydoxylated. Moreover, it turns out that the amount of hydroxy groups is small ($x < 0.1$), which confirms that the fluorolysis is the dominant reaction. Overall, as a very big surprise these hydroxy groups are Brønsted acidic in nature. Both bulk-surface techniques as well as the catalytic performance of these materials confirm this unusual result. The unexpected Brønsted acid character of the Mg–OH group on these magnesium fluoride surfaces is a result of the combination of different factors, as shown in Figure 8. First of all, fluorine is more electronegative than oxygen and hence induces additional electron withdrawal from Mg atoms, thus weakening the O–H bonds (Figure 8a). Moreover, the presence of undercoordinated magnesium sites further facilitates withdrawing of electron density from the

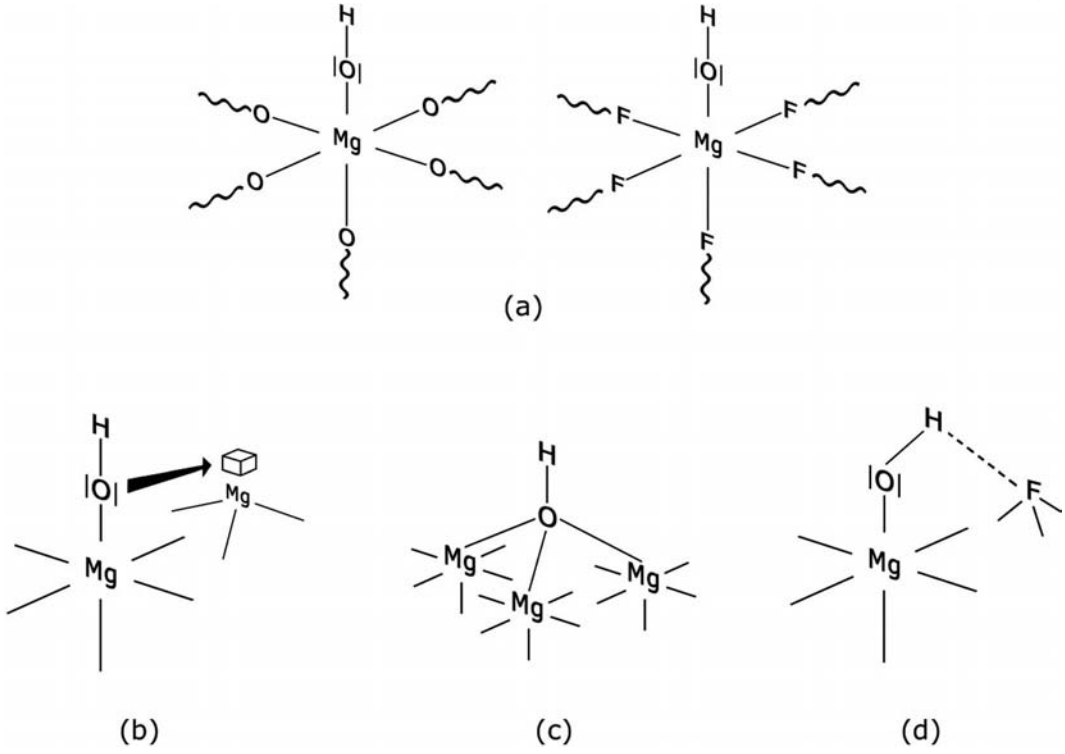

Figure 8. Graphical illustration of possible topological situations on the $MgF_{2-x}(OH)_x$ surface that could explain the Brønsted acidic nature of the OH group: (a) OH group on a MgO or MgF_2 surface, (b) interaction of an OH group with undercoordinated magnesium, (c) branched Mg–OH group and (d) hydrogen bonding between the H atom of the OH group and a F atom.[65]

O–H bond (Figure 8b). In addition, since fluorolysis and hydrolysis reactions proceed simultaneously, bridging OH groups at the surface may be formed in this way. Such groups would be stronger Brønsted acid sites than non-bridging ones (Figure 8c).[67] Last but not least, formation of hydrogen bonds between O atoms of an OH group and a neighbouring F atom are possible (Figure 8d), as was demonstrated for water adsorbed on MgF_2.[52] One key property for the Brønsted acidic behaviour of these OH groups is the small amount of these groups at the surface [$x < 0.1$ for $MgF_{2-x}(OH)_x$]. By using 20 wt.-% of aqueous HF (a Mg/HF ratio of 1:2), the hydrolysis becomes significant in comparison to the fluorolysis, and consequently Brønsted basic sites are present in the final sample.[65] Here, OH groups are at the surface and in the bulk, and the effects described in Figure 8 become less relevant; therefore, typical OH groups (basic) like those in MgO are formed.

Therefore, in the range from 100 wt.-% to 40 wt.-% aqueous HF, Brønsted acidic samples with different strength can be formed that have a constant ratio of Mg to HF. These samples possess very high surface areas ranging from 200 to 450 $m^2 g^{-1}$. Moreover, adsorption of CO reveals the presence of five- and fourfold-coordinated Mg^{2+} sites on the surface. This additional finding suggests that $MgF_{2-x}(OH)_x$ samples prepared by the sol–gel method are biacidic materials. The crystallization of these samples starts at around 220 °C and limits the catalytic application to 200 °C, which is totally sufficient for the production of fine chemicals, as shown below.

3.5. Support and Bifunctional Magnesium Fluorides

The synthesis of precious metal catalysts (M = Au, Pd and Pt) supported on magnesium fluoride follows synthesis protocols similar to those described for pure MgF_2 as well as for the magnesium oxide fluoride phases.

Impregnation Method

The easiest way to obtain $M@MgF_2$ catalysts is to first prepare sols of $MgF_{2-x}O_x$ in an alcohol solution and immediately add a suitable metal precursor like $HAuCl_4$, H_2PtCl_6 or $PdCl_2$ to deposit/impregnate the precious metals onto the nanoparticle surface. The alcohol causes immediate reduction of gold, while for Pd and Pt, passing hydrogen gas at slightly elevated temperature (78 °C) through the reaction system results in the reduced metallic state. In this way, precious metal catalysts finely dispersed on $MgF_{2-x}O_x$ phases were obtained that exhibited bifunctional catalytic properties.

The "incipient wetness impregnation" method was also used for the preparation of a new cationic gold catalyst supported on hydroxylated magnesium fluoride by using aqueous $HAuCl_4$ as metal precursor and the hydroxylated fluoride, $MgF_{2-x}(OH)_x$, as support.[68] The complete deposition of gold was achieved by filling the impregnation solution directly into the pores of the mesoporous $MgF_{2-x}(OH)_x$, the volume of the impregnation solution corresponding to the determined pore volume of $MgF_{2-x}(OH)_x$. There was no washing step or any other step during the incipient wet-

ness impregnation procedure in which a loss of gold could occur. In addition, because of the acidic pH of the impregnation solution (determined by the acidic character of the tetrachloroauric acid), there should be a strong electrostatic interaction between the gold complexes in the impregnation solution and active sites on $MgF_{2-x}(OH)_x$. The catalyst precursors were further calcined at 100 °C and 150 °C, and the resulting materials were denoted Au-100 and Au-150. The change in the chemical state of gold with the calcination temperature is shown by EXAFS spectra of the samples prepared and the "white line" (WL) of the Au L_3-edge absorption spectra (Figure 9). This absorption feature, in a range of a few eV above the edge, describes the electron transitions from the Au $2p_{3/2}$ core level to vacant d states, above the Fermi level. The WL is almost flat for metallic gold, for which the 5d states are completely occupied. However, for ionic compounds, the charge transfer from Au to the surrounding anions empties some of the 5d states and enhances the WL.[69] The sharp WL in the spectrum of sample Au-100 corresponds to the ionic Au–Cl bonds in the

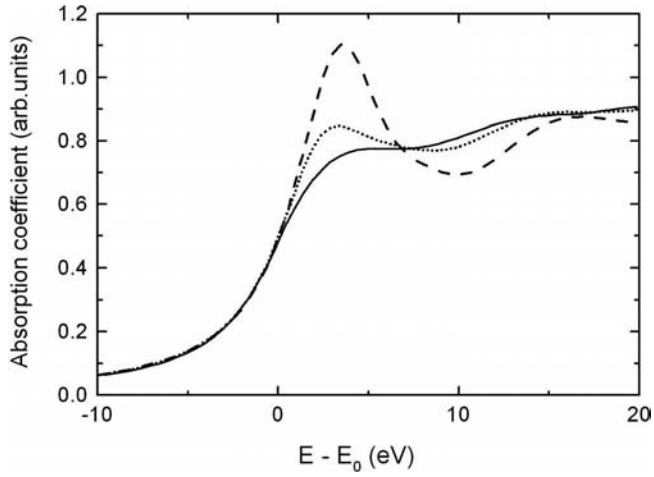

Figure 9. The Au L_3-edge white line of the absorption spectra of the Au foil (–) and the samples Au-100 (---) and Au-150 (···). Reprinted with permission from ref.[68] Copyright 2010 Wiley-VCH Verlag GmbH & Co. KGaA.

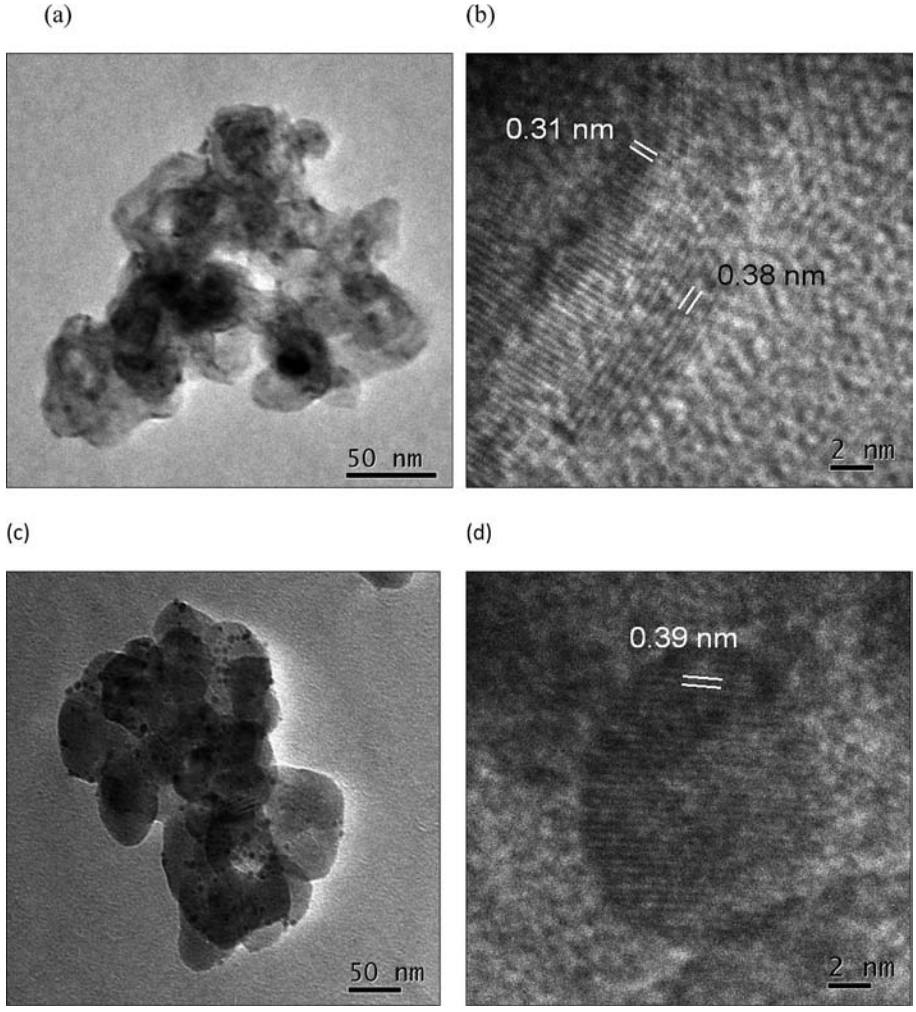

Figure 10. TEM images of fresh (a–b) and used (c–d) Pd^0/CaF_2 catalysts employed for hydrodehalogenation of $CHClF_2$.[72] Reproduced by permission of the Royal Society of Chemistry.

gold precursor, remaining essentially unchanged after the treatment at 100 °C. The temperature increase to 150 °C flattens the WL, as an effect of the partial reduction of gold to the metallic state, in agreement with the EXAFS results.[68] In fact, EXAFS measurements showed that this apparently small temperature difference is just sufficient enough to pass from small ionic gold particles to highly agglomerated metallic gold particles with a low-index surface, which are known to be inert[70] and inactive towards most molecules.

The formation of highly agglomerated gold particles was also observed in XRD diffraction spectra for the Au-150 sample. The same XRD technique showed that the amorphous state of the pure nanoscopic fluoride was successfully preserved. The novelty of the method also arises from the fact that the applied procedure did not require additional treatment with highly toxic compounds such as KCN or high-temperature activation steps, as usually needed for the generation of isolated cationic gold sites.

Bulk-Phase Incorporation

In a modified version of the former procedure, in a first step, the reaction of anhydrous hydrogen fluoride with the corresponding solutions of the metal alkoxides containing up to 10% $Pd(acac)_2$ yielded the catalyst precursors in the form of gels.[71,72] In a second step, gas-phase fluorination followed by H_2 treatment was employed to obtain the final Pd^0/MF_n catalysts. The characterization of the materials obtained revealed a uniform dispersion of Pd nanoparticles with a mean particle size of 5 to 8 nm (cf. Figure 10) inside the highly distorted MF_n structures characterized by moderate Lewis acidity as shown in Figures 11 and 12.

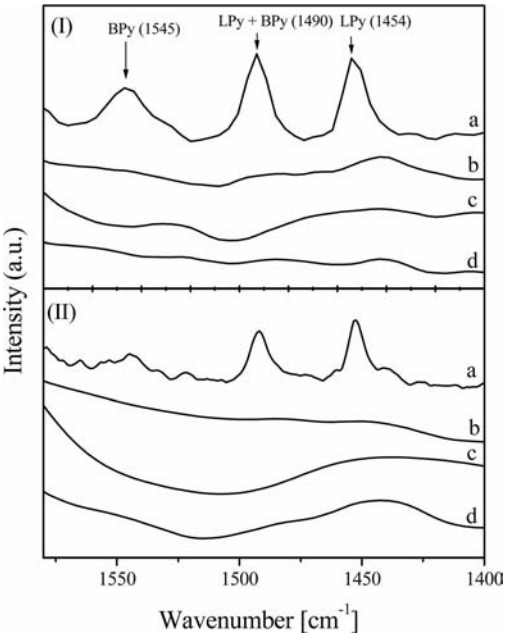

Figure 11. FTIR photoacoustic spectra of pyridine chemisorption of (I) MF_x (a: AlF_3; b: MgF_2; c: CaF_2 and d: $KMgF_3$) and (II) Pd^0/MF_x (a: Pd^0/AlF_3; b: Pd^0/MgF_2; c: Pd^0/CaF_2 and d: $Pd^0/KMgF_3$) samples.

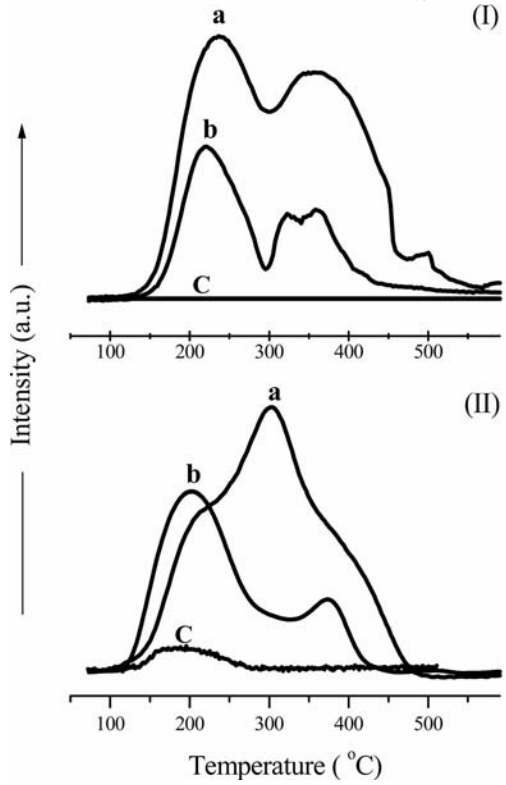

Figure 12. NH_3-TPD profiles of (I) MF_x (a: AlF_3; b: MgF_2 and c: CaF_2) and Pd^0/MF_x (II) (a: Pd^0/AlF_3; b: Pd^0/MgF_2 and c: Pd^0/CaF_2) catalysts.

4. Catalytic Applications of Fluorides

One of the most important fields of application for high-surface-area metal fluorides (HS-MF_n) is catalysis. The easy tuneability of their chemical properties from extremely highly Lewis acidic (e.g., HS-AlF_3)[4,73,74] to graded Lewis acidic (e.g., M^{3+}-modified MgF_2),[60–63] Lewis acidic and basic [e.g., Mg(O,F)][65] or biacidic (Lewis/Brønsted acidic) [e.g., Mg(OH,F)],[65,66,75–77] and the possibility to anchor and/or disperse other catalytically active materials upon each of this class of materials[68,78,79] (Scheme 2) opens new and unexpected opportunities for their application in heterogeneous catalysis for a large number of organic reactions to prepare a range of compounds from bulk chemicals to fine chemicals, intermediates and pharmaceutical products.

4.1. Base-Catalyzed Reactions

The catalytic potential of magnesium oxide fluoride materials prepared according to the *fluorolytic* sol–gel approach were first screened for the Michael addition of 2-methylcyclohexane-1,3-dione to methyl vinyl ketone (Scheme 3).[64]

Magnesium oxide fluorides with different fluorine contents were synthesized from the freshly prepared magnesium alkoxide by reacting it in a first step with the adjusted amount of anhydrous HF followed by addition of the amount of distilled water necessary to obtain the desired O/

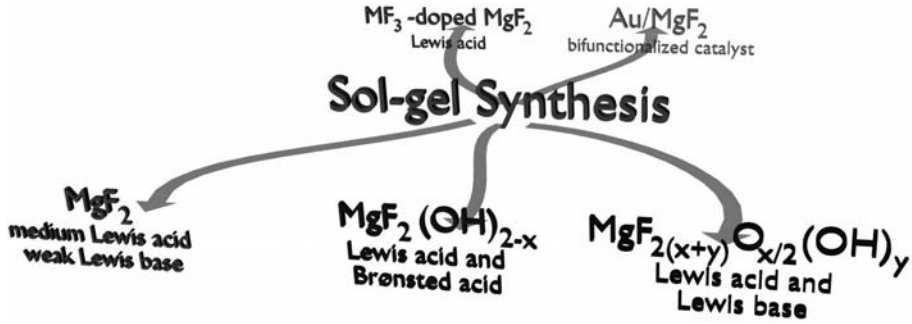

Scheme 2. Different functionalities of metal fluorides prepared by *fluorolytic* sol–gel synthesis.

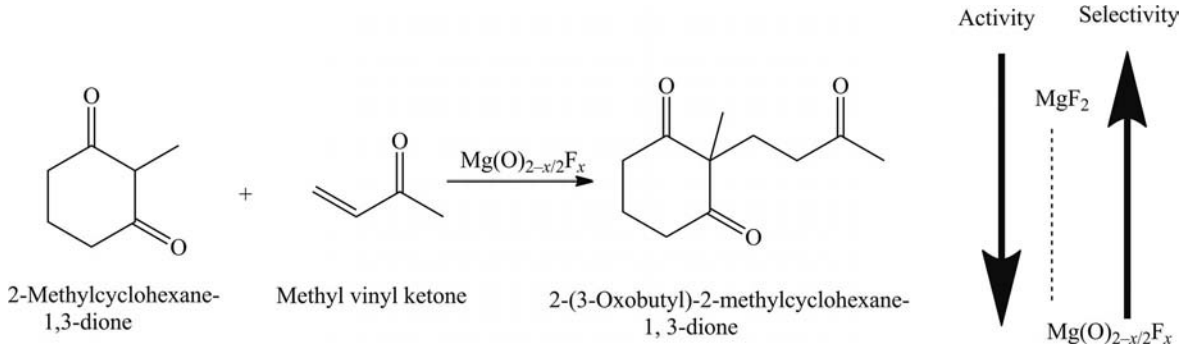

Scheme 3. Changing Lewis acidity/basicity by changing the F to O ratio in the $MgO_{2-x/2}F_x$ samples.

Mg mol ratio as described in Section 3.3. $MgO_{2-x/2}F_x$ samples (calcined at 350 °C and designated as "MgOF-X", where X indicates the stoichiometry of F related to Mg) were used as heterogeneous catalysts in Michael additions. The incorporation of F into the MgO network led to an increase in the Lewis acidity but at the same time a decrease in the Lewis basicity (Scheme 3 and Section 3.3.), as demonstrated above.

The catalytic behaviour of the MgOF samples and $Mg(OH)_2$ for the Michael addition of 2-methylcyclohexane-1,3-dione to methyl vinyl ketone is shown in Figure 13.

The pure, crystalline MgF_2 samples, c-MgF_2 and MgOF-2.5, were catalytically inactive. The other MgOF samples, MgOF-0 (MgO), MgOF-0.4, MgOF-1.2, MgOF-1.6, MgOF-2.0 (MgF_2) and commercially available $Mg(OH)_2$ exhibited diverse catalytic activities (Figure 12, left). MgOF-0 (MgO) showed very high catalytic activity for the Michael addition, similar to that found for MgO synthesized in aqueous medium. It gave a 70% yield of the Michael adduct in less than 1 h. After that, the yield gradually decreased to below 20% in 24 h; this was caused by the consecutive intramolecular aldol cyclization of the adduct. Commercial $Mg(OH)_2$ was slower to give a maximum Michael adduct yield of over 70% in 4 h, afterwards the yield decreased to 45% in 24 h. The different F contents of the samples, MgOF-0.4, MgOF-1.2, MgOF-1.6 and

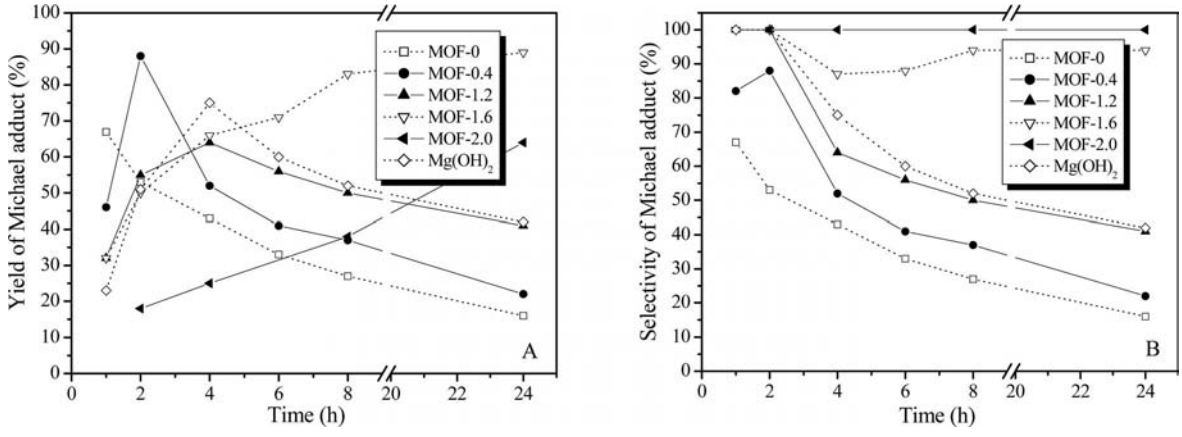

Figure 13. Michael addition of 2-methylcyclohexane-1,3-dione to methyl vinyl ketone with MgOF samples calcined at 350 °C. Yield (left) and selectivity (right) of Michael adduct vs. reaction time.[64] Reproduced by permission of the Royal Society of Chemistry.

MgOF-2.0 (MgF_2), have a direct influence on their catalytic activity and selectivity. The sample with the lowest fluorine content (MgOF-0.4) was the most active within this series and gave a high Michael adduct yield of about 90% after 2 h, which is similar to that with MgOF-0 (MgO), but the yield decreased to approximately 25% after 24 h. MgOF-1.2 exhibited a catalytic behaviour similar to that of $Mg(OH)_2$. The samples with higher fluorine contents, MgOF-1.6 and MgOF-2.0 (MgF_2), were less active, kinetically speaking (highest yields took longer to reach), but they gave Michael adduct yields of 90 and 65%, respectively, after 24 h. In contrast to MgOF-0.4 and MgOF-1.2, these catalysts yielded no consecutive products and were very selective (Figure 13, right).

In summary, the catalytic activity (based on the optimized strength of the basicity of the catalytic surface sites) decreases in the following order: MgOF-0 (MgO) > MgOF-0.4 > $Mg(OH)_2$ > MgOF-1.2 > MgOF-1.6 > MgOF-2.0 (MgF_2) (Figure 13, left); the selectivity decreases in almost the exact opposite order: (MgF_2) MgOF-2.0 > MgOF-1.6 > $Mg(OH)_2$ MgOF-1.2 > MgOF-0.4 > MgOF-0 (MgO) (Figure 13, right). These results demonstrate the directed tuning of the basicity of magnesium oxide fluorides by the fluorine content and presence of hydroxy groups.

With three further CH acids (pK_a values), 2-acetylcyclopentanone (7.8), 2-acetylcyclohexanone (10.1) and 2-methoxycarbonylcyclopentanone (10.3), similar to the reaction with 2-methylcyclohexane-1,3-dione to methyl vinyl ketone, high product yields of 75–90% with 100% selectivity were obtained after 24 h. As expected, the reaction was fastest for the addition of the CH acid with the lowest pK_a value, 2-acetylcyclopentanone.

4.2. Reactions Catalyzed by Lewis Acids

For some reactions, the Lewis acid sites of the catalyst might be too strong, as for instance in case of the Lewis acidic HS-AlF_3 catalyst,[80] which displays very high activity in CCl_2F_2 dismutation but no catalytic activity in $CHClFCF_3$ dismutation. The latter reaction occurs via elimination–addition of HF.[81] Thus, HF formed in the elimination step is strongly attached to the strong Lewis acid sites of HS-AlF_3, in this way blocking the catalytically active centres and preventing any catalytic reaction below 300 °C (temperature at which desorption of HF starts). On the other hand, HS-MgF_2 synthesized accordingly is a too weakly Lewis acidic catalyst for organic reactions, while conventionally prepared MgF_2 exhibits no Lewis acidity at all.[60] Doping of MgF_2 with different metals is an alternative option to overcome such problems. In this way, the Lewis acidity can be created by preparing host–guest metal fluoride systems in which a minor component, the guest, is distributed into the major component, the host, whereby the metal ions of the minor component are expected to occupy places of those of the major one.[4,81] Such structures can be prepared if the ionic radii of the host and the guest metal ions lie within a deviation range of approximately 15%, which results in a homogeneous distribution of the MF_n guest in the magnesium fluoride host system. This has been successfully proven in studies in which Fe^{3+}, Cr^{3+}, V^{3+}, Ga^{3+} and In^{3+} were used as guest ions.[61–63] Additionally, the soft-chemical nonaqueous *fluorolytic* sol–gel route applied to such mixed metal fluorides gives access to mesoporous (30–80 Å diameter) solids with high surface areas up to about 200 $m^2 g^{-1}$ and even larger.

While the Lewis acidity of HS-AlF_3 is too strong to be suitable for reactions such as Friedel–Crafts benzylation, acylation and alkylation because of the formation of unwanted side-reactions, the Lewis acidity created in Fe^{3+}/MgF_2, Ga^{3+}/MgF_2 and In^{3+}/MgF_2 catalysts has been advantageously used for the above syntheses.[61–63] Moreover, such materials display high activity in industrially interesting reactions like halogen exchange, hydrofluorination and dismutation.[62,63]

The advantages of such host–guest systems will be shown for the Fe^{3+}/MgF_2 system to present an example. This is a two-step nonaqueous synthesis (Figure 5) from different Fe^{III} precursors and $Mg(OCH_3)_2$, in which the second step is an activation by a postfluorination with either a chlorofluorocarbon or HF. This procedure leads to a material with higher Lewis acidity than the pure host system (MgF_2) and good catalytic activities in several organic reactions[61] such as:

(1) hydrofluorination of tetrachloroethene [Equation (5)]:

$$n Cl_2C{=}CCl_2 + m HF \rightarrow CF_3CHCl_2 + CF_3CHClF + CF_3CHF_2 + \text{others} \quad (5)$$

(2) dismutation of CCl_2F_2 [Equation (6)]:

$$2CCl_2F_2 \rightarrow CCl_3F + CClF_3 \quad (6)$$

(3) benzylation of anisole [Equation (7)]:

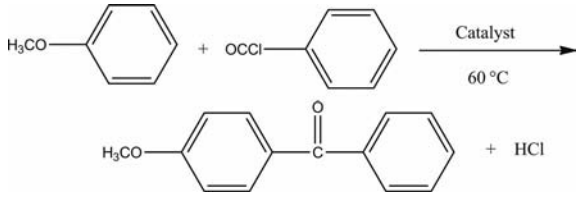

(7)

and

(4) alkylation of benzene with isopropyl chloride [Equation (8)]:

$$C_6H_6 + C_3H_7Cl \rightarrow C_6H_5{-}C_3H_7 + HCl \quad (8)$$

It is well known that heterogeneously catalyzed hydrofluorination reactions require Lewis acid sites.[82] However, as a result of the presence of HF in the reaction, the strongest Lewis acid sites can interact with HF ($M^{3+}\cdots$F–H surface complexes), resulting in blockage of these Lewis sites, thus transforming them into Brønsted acid sites. As a consequence, the catalytic hydrofluorination activity is reduced.[62] This hypothesis was confirmed by an only negligibly low catalytic hydrofluorination activity of a Fe^{3+}/MgF_2 catalyst prepared from $Fe(OCH_3)_3$ as precursor and post-

fluorinated with CFC-12, which had been proven to be the strongest Lewis acid material of the discussed Fe^{3+}-doped MgF_2 catalysts obtained from different Fe precursors.[62]

The dismutation of CCl_2F_2 [Equation (6)], often used as a probe reaction to determine the strength of the Lewis acidity of fluoride-based catalysts, confirms the advantage of organic precursors for obtaining solid Lewis acidic catalysts of high acid strength, as it has been reported for HS-AlF_3, which was prepared from an aluminium isopropylate precursor.[8] Therefore, with the Fe^{3+}/MgF_2 catalyst obtained from an iron methoxide precursor and postfluorinated (activated) with CFC-12, the dismutation took place with higher conversion (89% at 350 °C and 25% at 150 °C) than that with the catalyst sample prepared from iron chloride precursor and postfluorinated with CFC-12 (25% at 350 °C).[62]

Because of their substantial Lewis acidity, the Fe^{3+}/MgF_2 catalysts were also tested for their potential as substitutes for classically used Lewis acids such as $AlCl_3$ and $FeCl_3$. The catalysts have shown almost 100% conversion of benzoyl chloride with 60–80% selectivity for 4-methoxy benzophenone in a liquid-phase benzoylation reaction [Equation (3)]. As in the above examples, the most promising systems were obtained from $Fe(OCH_3)_3/Mg(OCH_3)_2$ precursors postfluorinated with HF instead of CFC-12.

To alkylate a nonactivated aromatic ring compound, the reaction of benzene with isopropyl chloride [Equation (8)] was investigated in a closed glass vessel at room temperature in the presence of Fe-doped magnesium fluoride catalysts.[61] In a short reaction time, a conversion of 100% was achieved by yielding 84% isopropyl benzene.

The same nonaqueous synthesis route turned out to be a powerful tool for the preparation of chromium(III)-doped magnesium fluoride, even though chromium alkoxides are not available. The prepared Cr^{3+}/MgF_2 systems exhibited quite high surface areas and an increased Lewis acidity due to the presence of low-coordinated Cr^{3+} sites introduced into the MgF_2 host.[63] Unlike the Fe^{3+}/MgF_2 catalysts, the postfluorination of oxidic Cr^{III} species with CFC-12 or with HF never resulted in pure chromium fluoride but almost always in chromium oxide fluoride species, which are not stoichiometric chromium oxide fluorides but phases with varying Cr/O/F ratios.[82–85]

The catalytic properties of differently doped Cr^{III} (8, 15 and 25wt.-%)/MgF_2 systems were tested in a flow system for the dismutation of CCl_2F_2 and CF_3CHClF. While the first reaction is used as a test reaction to determine the strength of the Lewis acidity of the catalytic material, the second reaction is of current industrial interest. For the dismutation of CCl_2F_2, the conversion increases with increasing temperature over the whole temperature range (100–350 °C) with all chromium-doped MgF_2 catalysts.[63] At 100 °C, the catalysts did not considerably differ in their performance (lowest: 0%; highest: 15%). In order to get a more significant differentiation, the reaction was performed at 350 °C. Here, the lowest conversion (with catalysts prepared from chromium chloride with 15 mol-% Cr with respect to Mg in the final sample) was 41%, and the highest one (with catalyst prepared from chromium(VI) oxide and 15 mol-% Cr with respect to Mg in the final sample) was 85%. The same order was found over the whole temperature range (Figure 14).

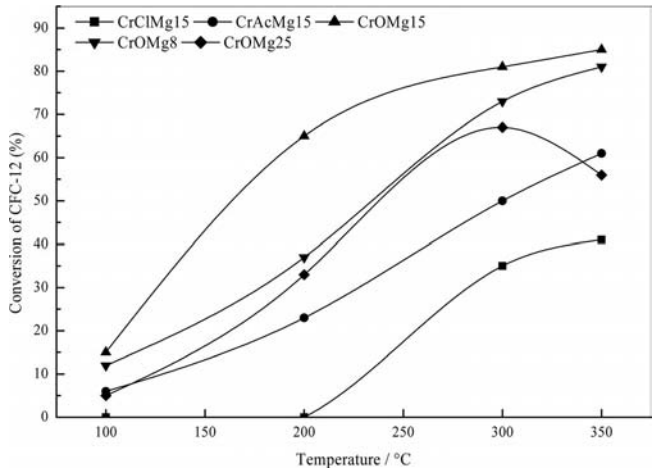

Figure 14. Dismutation of CCl_2F_2 over CrF_3/MgF_2 catalysts at t_R = 2 s; CCl_2F_2/N_2 = 1:5.[63] CrClMg15 designates catalysts with 15 mol-% Cr with respect to Mg in the final sample obtained from chromium chloride; CrAcMg15: obtained from chromium acetate; CrOMg15: obtained from chromium oxide; CrOMg8: sample with 8 mol-% Cr with respect to Mg in the final sample obtained from chromium(VI) oxide; CrOMg25: sample with 25 mol-% Cr with respect to Mg in the final sample obtained from chromium(VI) oxide. Reprinted from ref.[63] with permission from Elsevier.

The catalytic results obtained suggest that, in the case of chromium catalysts, "chromium oxide fluoride" species are the active sites. Under the nonaqueous *fluorolytic* synthesis conditions, such oxide- or hydroxide fluoride species cannot be formed from chromium chloride. In contrast, a "chromium oxide fluoride" can be formed in the course of catalyst synthesis from chromium oxides as well as basic chromium acetate. On the other hand, the data obtained on CrOMg confirm once again the well-known fact that an amount of 15–20% of the dopant has the highest effect.[60] A higher dopant concentration causes almost a segregation of the pure dopant phase. Hence, the segregation of pure chromia phase may cause the drop in activity observed in Figure 14.

In correlation with FTIR photoacoustic spectra of pyridine chemisorbed on surfaces of the solid support and various doped systems (see Section 3.2.), the calcined products of $GaF_3 \cdot 3H_2O$ and $InF_3 \cdot 3H_2O$ do not possess any Lewis acid sites.[61] This is also in accordance with their catalytic inactivity in chemical reactions such as dismutation and hydrofluorination.

As described by the Tanabe model,[60] when a trivalent cation is used as a dopant (guest) in a divalent metal fluoride, creation of Lewis acidity is expected as a result of the generation of an excess of local positive charge at the dopant metal atoms. Indeed, Ga^{3+}-doped MgF_2 displays a considerable Lewis acidity, which confirms, as in the other two previously described examples, that the combination of the host MgF_2 with the guest species GaF_3 generates Lewis

acidity.[61] Moreover, the acidity increases with increasing Ga^{3+} concentration in a way that the maximum catalytic activity was quite often found between guest concentrations of 15 and 20%. This corresponds well with experimental results for other systems such as V^{3+}- and In^{3+}-doped MgF_2 Lewis acid systems.[60]

Unlike Ga/MgF_2 samples, In^{3+}-doped MgF_2 catalysts exhibit lower Lewis acidity. This can be explained by the large difference in the ionic radii of Mg^{2+} and In^{3+}, which do not properly match as well as those of Mg^{2+} and Ga^{3+}.[60] The catalytic activity of these samples in the dismutation reaction of CCl_2F_2 [Equation (6)] is presented in Figure 15.

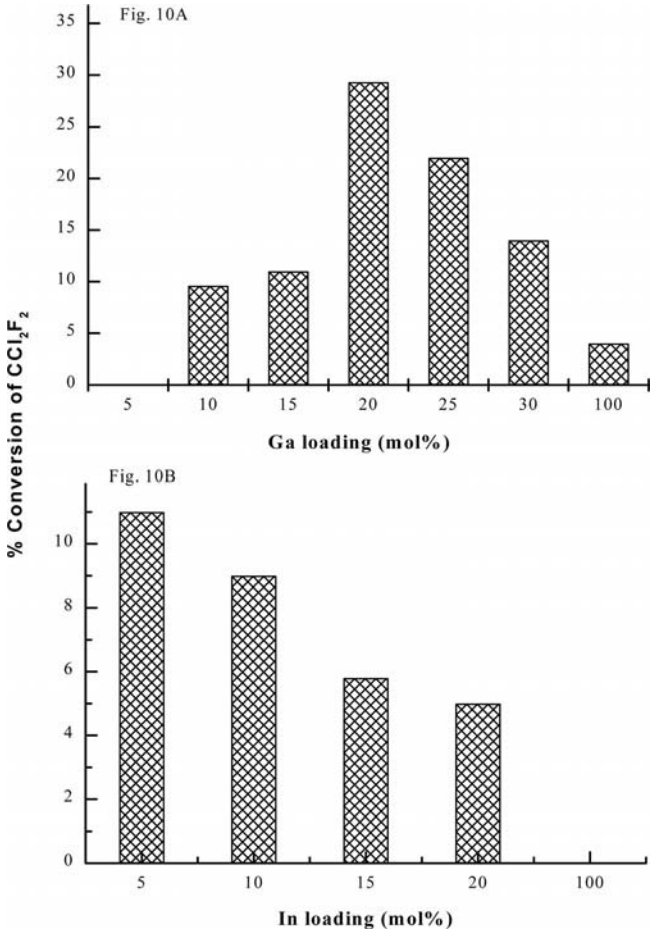

Figure 15. (A) Catalytic activity of Ga^{3+}-doped systems in the CCl_2F_2 dismutation reaction. (B) Catalytic activity of In^{3+}-doped systems in CCl_2F_2 dismutation reactions. Reprinted from ref.[61] with permission from Elsevier.

As Figure 15A shows, a GaF_3-doped MgF_2 catalyst with 5% Ga^{3+} does not display any activity, but with increasing Ga^{3+} concentration, the conversion of CCl_2F_2 reaches about 30% at 20% Ga^{3+}. Further increase in the Ga^{3+} concentration results in decreasing conversion (Figure 15A). In contrast, the best catalytic activity for the In^{3+}-doped MgF_2 was obtained for 5% In^{3+} (Figure 15B).

The presented catalytic results certainly prove that, even though the nonaqueous *fluorolytic* sol–gel synthesis route for doped metal fluorides was explored just a few years ago, remarkable progress has been achieved in the meantime by investigating them under laboratory conditions. Nevertheless, despite all progress already achieved, there will be a lot of important organic reactions waiting to be tested, both from the basic scientific as well as from the application points of view.

4.3. Biacidic Lewis and Brønsted Metal Fluoride Catalysts

To increase the range of the catalytic application of *fluorolytic* sol–gel metal fluorides, we also need to consider reactions that require catalysts with Brønsted acid surface sites. As we have shown in previous sections, for those reactions we have further developed the application of the *fluorolytic* sol–gel synthesis route in order to access a new class of biacidic heterogeneous catalysts. In this context, a novel approach will be presented that results in Lewis and Brønsted acidic materials[65,66,75,76] by combining the *fluorolytic* and the *hydrolytic* sol–gel syntheses, as described in Section 3.4.

When a metal alkoxide is reacted with stoichiometric amounts of aqueous HF, a competition between fluorolysis (resulting in M–F formation) and hydrolysis (resulting in M–OH formation) has to be expected, resulting in the formation of hydroxide fluorides. The hydroxy groups are surprisingly not basic in nature, as might be expected for Mg–OH groups, but Brønsted acidic. Thus, Lewis acid sites (under coordinated metal sites) and Brønsted acid sites (M–OH groups) are formed. Both types of acid sites (Brønsted/Lewis) can be tuned by applying different molar ratios of HF to H_2O during sol–gel synthesis.[66,75] The materials obtained have been successfully applied to the synthesis of vitamin E [(all-*rac*)-α-tocopherol], vitamin K_1 and K_1-chromanol,[65,66,75,76] the Friedel–Crafts alkylation of aromatic compounds, including that of benzene to ethylbenzene with benzyl alcohol as alkylating agent,[77] and the highly diastereoselective synthesis of (±)-isopulegol [precursor for (±)-menthol].[75]

(all-*rac*)-α-Tocopherol (vitamin E) displays important antioxidant properties and shows promising results in the prevention and treatment of heart disease, cancer and Alzheimer's disease.[86–88] As it is also used in high amounts in other important industrial markets, the demand for (all-*rac*)-α-tocopherol is constantly increasing.[89] The synthesis of this valuable compound, made by the condensation of 2,3,6-trimethylhydroquinone (TMHQ, **1**) with isophytol (IP, **2**), possibly proceeds through Friedel–Crafts alkylation–cyclization (Scheme 4)[90–97] or through the *ortho*-Claisen rearrangement of an intermediary allyl ether (Scheme 5).[98,99]

Even though only in small amounts, the formation of byproducts was also observed when a strong Lewis/Brønsted acidic fluoride (e.g., hydroxylated AlF_3) was used as catalyst.[100] Some of the observed intermediates and byproducts, which are also known from the literature,[101] are presented in Scheme 6. To the best of our knowledge, quinone **9** was not claimed until now in the literature for this synthesis.

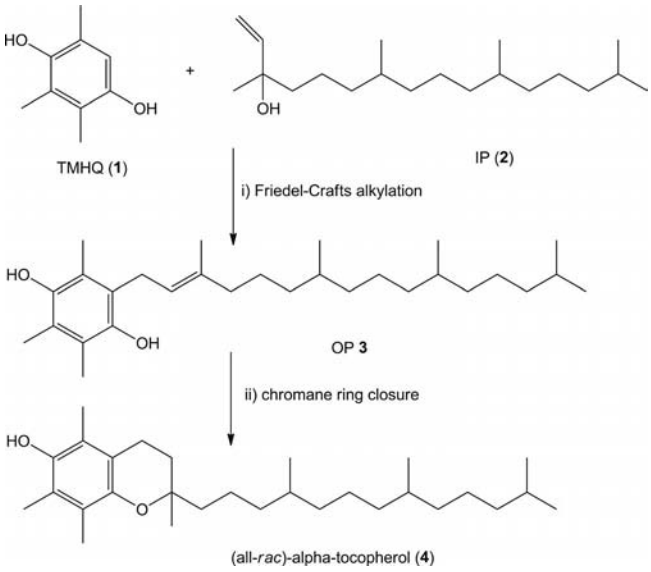

Scheme 4. The synthesis of (all-*rac*)-α-tocopherol by the condensation of 2,3,6-trimethylhydroquinone (TMHQ, **1**) with isophytol (IP, **2**) through Friedel–Crafts alkylation–cyclization.

When nanoscopic hydroxylated magnesium fluorides were employed as catalysts, complete conversion of IP (**2**) was accomplished in less than 1 h, and the desired product was obtained with selectivities in the range 76.3–87.0% depending on the nature of the catalyst (Table 2). In comparison, commercial crystalline MgF_2 (MgF_2-C, Table 2, entry 1) proved not to be active at all in this synthesis of (all-*rac*)-α-tocopherol (**4**), because of its chemically almost inert surface. Samples with predominant Brønsted acid character (e.g., MgF_2-40 and MgF_2-57) showed excellent catalytic activity, but (all-*rac*)-α-tocopherol (**4**) was obtained in less than 83% yield. On the other hand, Lewis acid sites of moderate strength (e.g., in MgF_2-87 and MgF_2-100) seem not to be sufficient to promote the synthesis of (all-*rac*)-α-tocopherol (**4**), and IP (**2**) remains completely unconverted even after 5 h. It seems that the optimal combination of Lewis/Brønsted acid sites was generated in sample MgF_2-71, where (all-*rac*)-α-tocopherol (**4**) was obtained in highest yields (87%; Table 2, entry 4).

Table 2. Influence of the key surface features and the reaction parameters[a] on the catalytic performance.[66]

Entry	Catalyst	Number of acid sites per m^2	IP/catalyst mol ratio	*t* (min)	Tocopherol (% yield)
1	MgF_2-C	n.d.	n.d.	1800	0
2	MgF_2-40	5.4×10^{17}	119	300	76.3
3	MgF_2-57	6.6×10^{17}	76	300	82.6
4	MgF_2-71	3.6×10^{17}	123	300	87.0
5	MgF_2-87	4.8×10^{17}	60	360	0
6	MgF_2-100	8.4×10^{17}	37	360	0

[a] Reaction conditions: 50 mg catalyst; T = 100 °C; TMHQ/IP = 1:1; solvent: heptane/propylene carbonate = 50:50. Conversion is based on IP (C = 100%).

Alcohols, especially tertiary allylic alcohols such as IP (**2**), easily lose water in the presence of acids to form highly reactive carbocations. Therefore, the formation of considerable amounts of dehydration products, so-called phytadienes **10**, is a general problem in such procedures. A practical way to avoid these byproducts is to use the generally adopted procedure, in which IP (**2**) is added dropwise to a stirred mixture of the catalyst and TMHQ (**1**) dissolved in a suitable solvent.[102] However, we only found small amounts of phytadienes **10** (generally <5%) when TMHQ (**1**) was treated with IP (**2**), even if the latter was added from the beginning of the process in one single charge. This behaviour was probably due to the moderately strong acidity of the fluoride catalysts, which results in a low capacity for stabilization of the carbocation and thus in lower amounts of phytadienes **10**. Surprisingly however, the synthesis took place with complete regioselectivity, as long as no benzofuran derivatives were detected in the reaction products. Generally speaking, the regioselectivity of a catalytic reaction depends on the structure of the molecule, the

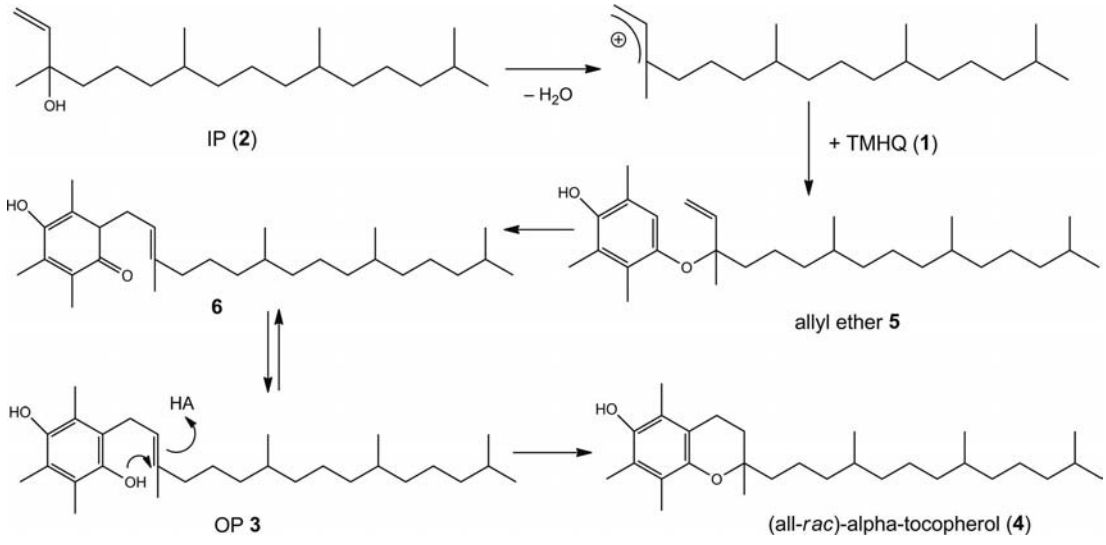

Scheme 5. The synthesis of (all-*rac*)-α-tocopherol by *ortho*-Claisen rearrangement of intermediary allyl ether **5**.

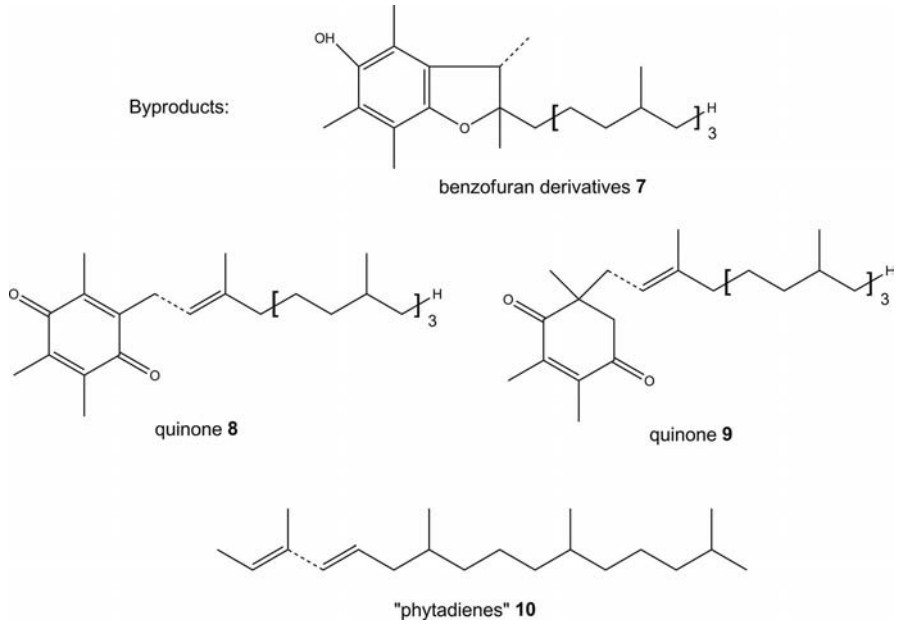

Scheme 6. Byproducts identified in the synthesis of (all-*rac*)-α-tocopherol (**4**).

structure of the catalyst, and the reaction conditions, all these factors being highly interdependent. In other words, a comprehensive interpretation of regioselectivity requires the substrate–catalyst couple to be considered as a supramolecular system. Particularly in the condensation of TMHQ (**1**) with IP (**2**), the availability and proportion of the different carbocations, for example isophytil and *n*-phytil that are formed by the interaction of IP (**2**) with the catalyst, seems to be the key feature for obtaining high regioselectivity of the desired (all-*rac*)-α-tocopherol (**4**). No quinone compounds **8** and **9** were detected even when reactions were conducted in vessels open to the atmosphere. Another important aspect could be that a different reaction mechanism to *ortho*-pulegol (OP) **3** (Schemes 4 and 5) has to be considered. Commonly, syntheses of (all-*rac*)-α-tocopherol reported in the literature proceed by the condensation of 2,3,6-trimethylhydroquinone (TMHQ, **1**) with isophytol (IP, **2**) through Friedel–Crafts alkylation–cyclization (Scheme 4). However, the combination of Lewis and Brønsted acid sites could favour an *ortho*-Claisen rearrangement (Scheme 5), which would also explain the absence of the usual byproducts observed with other catalysts. Unfortunately, detailed mechanistic studies of (all-*rac*)-α-tocopherol synthesis have not been performed so far, even though this reaction is very important for the society.

Another important process in which these new hydroxylated magnesium fluoride catalysts have the potential of bringing new impact to syntheses with heterogeneous catalysts is the synthesis of vitamin K_1, an important compound to control blood clotting.[76] The synthesis involves as a key step the Friedel–Crafts alkylation of menadiol acetate (MDA, **12**) with isophytol (IP, **2**), followed by the oxidation of dihydro-vitamin K_1.[103] Moreover, in a similar way to that in the synthesis of (all-*rac*)-α-tocopherol (**4**), alkylated intermediate **14** may lead to vitamin K_1-chromanol **13** through a cyclization step (Scheme 7).[76] It was shown that the effect of vitamin K_1 (**15**) on a number of biochemical processes (blood coagulation, conjugate oxidation, phosphorylation) is caused by K_1-chromanol **13** {naphthotocopherol or 2,5-dimethyl-2-(4,8,12-trimethyltridecan-1-yl)-6-hydroxybenzo[*h*]chroman}, identified in the product of the enzymatic reduction of vitamin K_1 (**15**). Chemical conversion of vitamin K_1 (**15**) to K_1-chromanol **13** was achieved with tin(II) chloride.[104] Spectrophotomet-

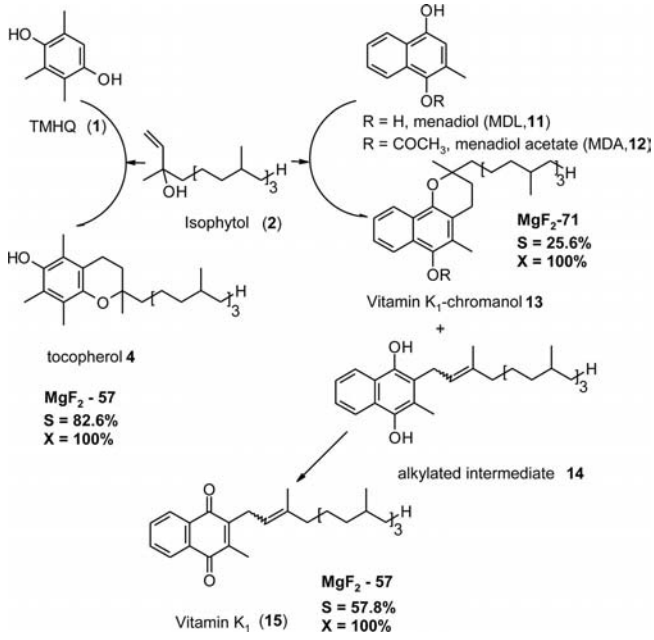

Scheme 7. The synthesis of vitamin K_1 (**15**) and K_1-chromanol **13** (the reaction paths are compared with the reaction path for the synthesis of tocopherol **4**). Adapted with permission from ref.[76] Copyright 2010 Wiley-VCH Verlag GmbH & Co. KGaA.

ric studies of antioxidants in the phenol series confirmed that the highest activity was with naphthotocopherol, whose antioxidant activity was seven times that of α-tocopherol.[105]

As shown in Scheme 7, a combination of a high density of moderately strongly Brønsted acidic sites and a low amount of moderately strongly Lewis acidic sites (e.g., MgF_2-57) favours the formation of vitamin K_1 (**15**) in relative high yields (57.8%). Taking into account that vitamin K_1 (**15**) is commercially produced in yields of 60–70% in the presence of liquid $BF_3{\cdot}OEt_2$ as catalyst, the obtained results are very encouraging from an environmental point of view.

Diphenylmethane and its derivatives are industrially important compounds used as pharmaceutical intermediates,[106] fine chemicals[107] and components in the fragrance industry.[108] Their synthesis is traditionally performed by using H_2SO_4, HF, $AlCl_3$, $FeCl_3$ or $ZnCl_2$[109] as acid catalysts. To avoid the use of homogeneous catalysts, Lewis acids have been supported on different solids, such as MCM-41,[110] hydroxyapatite (HAP),[111] and fluorapatite (FAP) and were used as heterogeneous catalysts for the Friedel–Crafts reaction of benzyl chloride with benzene and its derivatives. Unfortunately, the use of benzyl chloride as the alkylating agent, generating hydrogen chloride as byproduct, is undesirable from the green chemistry point of view. More appropriate is the use of benzyl alcohol, which generates only water as byproduct. Hence, there is still a need to develop an easy and clean technology that is more suitable for the synthesis of diphenylmethane and its derivatives. An alternative green solution to this problem could be the use of the partly hydroxylated, nanoscopic fluorides (MgF_2 and AlF_3) as catalyst and benzyl alcohol as alkylating agent under solvent-free conditions.[77]

The best results obtained in the alkylation of benzene (Scheme 8) are summarized in Table 3. TOF values are given as the number of benzyl alcohol molecules transformed per hour at the acidic sites, as calculated from measurements of NH_3–TPD and N_2 sorption isotherms.

The benzylation of aromatic hydrocarbons with benzyl alcohol in the liquid phase proceeded under relatively mild conditions with moderate activities and selectivities to diphenylmethane (DPM) and its derivatives. As shown in Table 3, the etherification of benzyl alcohol to dibenzyl ether (DBE) was much faster than the benzylation of the substrate. The selectivity for the main benzylation product could not be improved above 15% irrespective of the ratio of Brønsted/Lewis acid sites, which suggests a limitation of the capability of the catalyst in this kind of reactions. Nevertheless, the porosity of the MgF_2-57 catalyst and the density of its acid sites enabled the selectivity for the *para* isomer to be almost quantitative.[77]

Table 3. Conversion of benzyl alcohol and selectivity for diphenylmethane under different reaction conditions[a] as a function of catalyst nature and reaction conditions.[77]

Entry	Catalyst	*T* (°C)	**a**/BA mol ratio	*C* (wt.-%)	TOF (h^{-1})	*S* (wt.-%) DPM	*S* (wt.-%) DBE
1	MgF_2-57	100	1:2	11.1	1.8	3.5	96.5
2	MgF_2-57	100	4:1	12.6	1.0	11.7	88.3
3	MgF_2-57	120	4:1	38.2	3.1	14.5	85.5
4	MgF_2-71	100	1:2	17.5	4.5	2.7	97.3
5	MgF_2-71	100	4:1	18.4	2.35	10.1	89.9
6	MgF_2-71	120	4:1	42.0	5.4	13.2	86.8

[a] Reaction conditions: 100 mg catalyst, 24 h.

Another interesting and industrially important application in which the nanosized hydroxylated magnesium fluorides [$MgF_{2-x}(OH)_x$] were employed for the first time is the cyclization of citronellal to (±)-isopulegol [intermediate for the synthesis of (±)-menthol, Scheme 9, route 1A]. The investigated fluoride catalysts led to unexpected diastereoselectivities (91.7% for hydroxylated AlF_3 and 84.7% for hydroxylated MgF_2-71) superior to those of most conventional catalysts used for this reaction (71–75%). The catalytic efficiency seems to be influenced not only by the acidic properties but also by the textural properties of the catalyst.[75] However, by combining the acid function of the hydroxylated magnesium fluoride catalyst with the hydrogena-

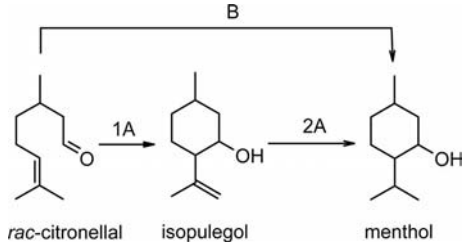

Scheme 9. The synthesis of menthol from citronellal in two steps (route 1A +2A) and in one pot (route B).

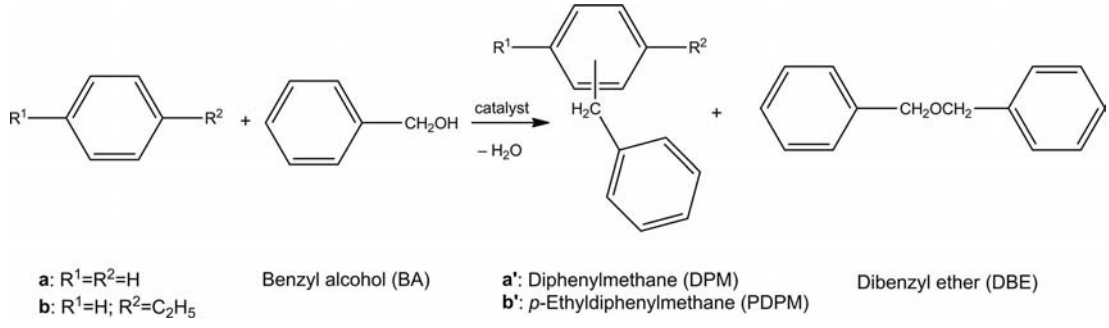

Scheme 8. Friedel–Crafts reaction of benzene and ethylbenzene with benzyl alcohol.[77]

tion activity of cationic gold nanoparticles, we could successfully present a Au/MgF_2 bifunctional catalyst.[68] This material is able to catalyze both steps of the synthesis of (±)-menthol (Scheme 9) in a diastereoselective one-pot procedure that will be discussed in the following section.

4.4. Bifunctionally Catalyzed Reactions

As it was shown in the previous section, with nanoscopic binary metal fluorides prepared by the sol–gel method, pure Lewis acidic as well as biacidic metal fluorides of different strengths are accessible, which can be applied in a large number of organic reactions.

When other catalytically active materials are anchored and/or dispersed in/on this class of materials, new bifunctional catalytic systems can be created.[42] Therefore, magnesium fluoride was applied as a support for systems containing individual oxides of transition metals (Mo, V, W, Cu, Cr) and then two different oxide phases (Cu–Cr, Cu–Mn), a metal phase (Ru, Pd) or heteropolyacids. The MgF_2-supported catalysts obtained in this way are characterized by high activity and selectivity in processes such as: hydrodechlorination of chlorofluorocarbons (CFCs), hydrodesulfurization of organic compounds and purification of fuel combustion products from nitrogen oxides.

The highlight of a bifunctional metal fluoride catalyst is the synthesis of gold/ hydroxylated magnesium fluoride for a one-pot synthesis of (±)-menthol (Scheme 9). The "incipient wetness impregnation" of the above hydroxylated magnesium fluorides (Section 3.4.) with hydrogen tetrachloroaurate as the gold precursor resulted in a new bifunctional ionic gold (4 wt.-%)/magnesium fluoride catalyst [for simplicity the hydroxylated fluoride $MgF_{2-x}(OH)_x$ will be simply referred to as "fluoride" or "MgF_2"], which can serve in the highly diastereoselective one-pot synthesis of (±)-menthol from citronellal (Scheme 9, route B).[68] This catalyst provides unexpectedly active ionic gold species for the selective hydrogenation of isopulegols to menthols. At the same time, the catalytic features of fluoride responsible for the diastereoselective isomerization of citronellal to (±)-isopulegol are preserved.

Interesting is also the fine line between a highly active and diastereoselective catalyst and a totally catalytically inactive material, imposed by a difference of only 50 °C in the calcination temperature (from 100 to 150 °C). In fact, as EXAFS measurements showed, this apparently low temperature difference is just enough to pass from small ionic gold particles to high agglomerations of metallic gold particles with low-index surfaces, which are known to be inert[70] and inactive towards most molecules.

By comparing the ionic-gold-based catalyst with Ir-based catalysts,[112] it was found that the former is totally selective to menthols (no byproducts such as citronellol, 3,7-dimethyloctanol, and 3,7-dimethyloctanal were observed), suggesting a different reaction mechanism (Scheme 10).

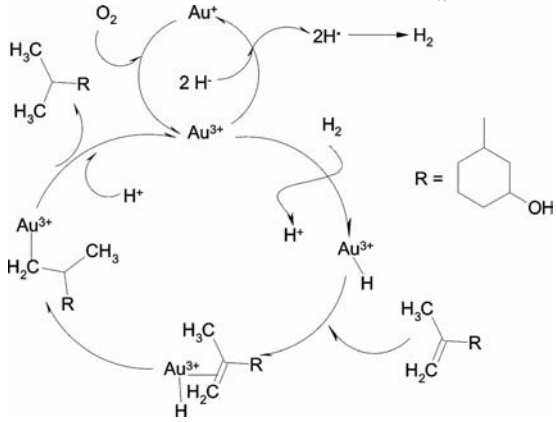

Scheme 10. Proposed catalytic cycle in the hydrogenation step of isopulegol to (±)-menthol with ionic gold particles. Reprinted with permission from ref.[68] Copyright 2010 Wiley-VCH Verlag GmbH & Co. KGaA.

In agreement with the previous work of Comas-Vives et al.,[113] with the ionic gold based catalyst the heterolytic cleavage of H_2 is more probable than its homolytic activation. These authors proved that the heterolytic cleavage of hydrogen requires a polar environment provided by the solvent. We have found that the heterolytic activation of hydrogen is favoured by the hydroxylated MgF_2 support; the proton remains on the polar surface whereas the hydride is bonded to the gold site. Thus, this novel catalyst can be used to perform such reactions in nonpolar solvents like toluene. However, the reduction of active Au^{III} to the inactive Au^{I} species accompanies the hydrogenation cycle. In order to regenerate the active Au^{III} species, Au^{I} must be reoxidized either through the generation of H^+ in the media or more effectively by air. Therefore, after a reaction time of 22 h the selectivity for (±)-menthol reaches 43%, and the diastereoselectivity in the formation of the isopulegols in the first step is preserved to a ratio of 87.8:12.2 (±)-isopulegol/(±)-neo-isopulegol, characteristic for the MgF_2 support.[75] When the catalyst was removed by filtration, dried in air at room temperature, and reintroduced for another 16 h, the selectivity for menthol improved to 60.8% showing a reoxidation of the gold Au^{I} particles to the Au^{III} oxidation state upon contact with air. A further reoxidation in air at room temperature of the catalyst improved the selectivity for (±)-menthol to 92.5%. This mechanism is less probable when large agglomerated metallic Au^0 particles are present, since they cannot participate in a spontaneous electron-transfer processes.

The obtained results may have important implications for the synthesis of other gold/porous material catalysts and their application as bifunctionalized catalysts. In addition, the Au/MgF_2 catalyst may also be applied to other reactions requiring both acid and hydrogenation activity.

The presented catalytic results support the unique behaviour of nanoscopic hydroxylated fluorides, not only as potential catalytic materials, but also as potential supports for active catalytic functions. Irrespective of the synthesis approach, the use of hydroxylated fluorides as catalysts offers

not only improved efficiency but also additional green elements, in complete agreement with the actual tendencies of 21th century chemistry.

5. Conclusion

The *fluorolytic* sol–gel synthesis of nanoscopic metal fluorides has been established as a valuable tool for accessing new materials with interesting properties and can, in the meantime, be regarded as powerful as the classical *hydrolytic* sol–gel synthesis route for metal oxides. Moreover, by combining the two synthesis approaches, new phases can be synthesized with unexpected catalytic activity as well as tuneability. This was already successfully demonstrated for systems based on magnesium fluoride as reported here and will be further extended in the future to other metal fluoride systems. Thus, the target is to establish a new class of tuneable acid–base catalysts for greener organic synthesis applications.

By the reaction of magnesium alkoxides with anhydrous hydrogen fluoride in alcohol solution, a wide variety of nanoscopic magnesium fluoride phases are accessible, and they represent new materials for very different applications. MgF_2 obtained in this way exhibits surface areas of up to 300 $m^2 g^{-1}$ and, importantly enough, a high amount of Lewis acid sites, which explain the different behaviour of this material in comparison to conventionally prepared MgF_2.

Modification of the synthesis opens very elegant routes to the formation of metal hydroxide fluorides or oxide fluorides by soft chemistry. This can be achieved in two different ways. The first approach uses an understoichiometric amount of HF during the first step of the synthesis followed by the addition of the stoichiometrically requested amount of water in order to complete the reaction. In this way, practically all compositions of $Mg(OH)_{2-x}F_x$ [$Mg(O_{6-x}F_x)$ octahedra] are accessible. By calcination, these hydroxide fluorides are transformed into the corresponding magnesium oxide fluorides ($MgO_{2-x/2}F_x$). By tuning the oxygen-to-fluoride stoichiometry inside these phases, the surface site character can be changed from being moderately Lewis acidic at high F content to being strongly Lewis basic at high oxygen content. Depending on the O/F ratio, these oxide fluoride phases preserve their amorphous character up to temperatures of about 600 °C and exhibit surface areas of up to 550 $m^2 g^{-1}$. Hence, these new materials are not only interesting as new catalytic phases but may also be of interest as supports for high temperature reactions. It is noteworthy to mention that these phases are thermally stable up to at least 1000 °C, which means that no notable hydrolysis or pyrolysis reaction takes place.

Another approach to obtain similar phases is the use of hydrofluoric acid with different water contents and adjusting the F/Mg stoichiometry to 2. In this way, the fluorolysis and hydrolysis reactions compete with each other, and since the fluorolysis is significantly faster, just partly hydroxylated fluoride phases with a very low OH content, which exhibit interesting acidic properties, are obtained. Surprisingly enough, partly hydroxylated magnesium fluoride [$MgF_{2-x}(OH)_x$ with $x < 0.1$] has Mg–OH groups that are not basic in nature but Brønsted acidic. In this way, solids are available that carry both Lewis and Brønsted acidic surface sites. Just by tuning the F/OH ratio inside the magnesium fluoride phases, the acid properties can be tuned from moderately strongly Lewis and Brønsted acidic to weakly Lewis acidic but decreasingly strongly Brønsted acidic (increasingly Brønsted basic).

It is noteworthy to mention that these catalytically interesting new materials can be used either as supports or as cocatalysts in combination with, for example, precious metals like Au, Pd, Pt.

As it has been shown with examples in this review, with pure materials based on magnesium fluoride and especially with a large variety of $MgF_x(OH)_{2-x}$ and $MgO_{2-x/2}F_x$ phases, a new class of potential catalysts has been explored. Their catalytic performances, already proven for several different reactions, encourage further exploration of these catalysts either in pure form or in combination with other catalytic species. Moreover, the extension to systems based on other metal fluorides is also very promising and will be the target of future work.

Acknowledgments

E. K. thanks the European Union for the support of part of this work through the 6th Framework Programme (FUNFLUOS, Contract No. NMP3-CT-2004-5005575). The Deutsche Forschungsgemeinschaft (DFG) (Ke-489/22, 28 and 29) and the Graduate School "Fluorine as key element" (GRK 1582) are also thanked for financial support. Furthermore, the impact of several former and present co-workers, who contributed at least partly to the content of this paper by their results, should be emphasized: Ying Guo, Katharina Teinz, Dr. Krisna Murthy Janmanchi, Dr. Sridana Shekhar, Dr. Zhijian Li, Dr. Udo Gross, Dr. Stephan Rüdiger, Dr. Pratap Patil, Dr. René König, Dr. Kerstin Scheurell, PD Dr. Gudrun Scholz, Dr. Detlef Heidemann, Dr. Anton Dimitrov, Mrs. Sigrid Bäßler. S. C. gratefully acknowledges a grant from the Alexander-von-Humboldt Foundation that initiated the joint work with E. K.

[1] G. Ertl, *Angew. Chem.* **1990**, *102*, 1258; *Angew. Chem. Int. Ed. Engl.* **1990**, *29*, 1219.
[2] P. Anastas, N. Eghbali, *Chem. Soc. Rev.* **2010**, *39*, 301.
[3] F. Schüth, *Angew. Chem. Int. Ed.* **2003**, *42*, 3604.
[4] S. Rüdiger, E. Kemnitz, *Dalton Trans.* **2008**, 1117.
[5] U. Groß, E. Kemnitz, *J. Fluorine Chem.* **2007**, *128*, 353.
[6] M. Niederberger, *Acc. Chem. Res.* **2007**, *40*, 793.
[7] L. L. Hench, J. K. West, *Chem. Rev.* **1990**, *90*, 33.
[8] E. Kemnitz, U. Groß, S. Rüdiger, S. C. Shekar, *Angew. Chem. Int. Ed.* **2003**, *42*, 4251.
[9] W. H. Bauer, A. A. Khan, *Acta Crystallogr., Sect. B* **1971**, *27*, 2133.
[10] G. Vidal-Valat, *Acta Crystallogr., Sect. B* **1979**, *35*, 1590.
[11] M. Jansen, J. C. Schön, *Angew. Chem. Int. Ed.* **2006**, *45*, 3406.
[12] M. A. C. Wever, J. C. Schön, M. Jansen, *J. Solid State Chem.* **1998**, *136*, 233.
[13] R. Hundt, J. C. Schön, A. Hannemann, M. Jansen, *J. Appl. Crystallogr.* **1999**, *32*, 413.
[14] M. A. C. Wever, J. C. Schön, M. Jansen, *J. Phys. Condens. Matter* **1999**, *11*, 6487.

[15] H. Putz, J. C. Schön, M. Jansen, *Comput. Mater. Sci.* **1998**, *11*, 309.
[16] J. C. Warf, W. C. Cline, R. D. Tevebaugh, *Anal. Chem.* **1954**, *26*, 342.
[17] L. Domange, *Ann. Chim. (Paris)* **1937**, *7*, 225.
[18] R. C. Weast (Ed.), *Handbook of Chemistry and Physics*, 59th ed., CRC Press, Cleveland OH, **1979**.
[19] E. Munia, C. B. Pedroso, A. B. Vilaverde, *J. Chem. Soc. Faraday Trans.* **1996**, *92*, 2753.
[20] M. Nofar, H. R. M. Hosseini, H. A. Shivaee, *Infrared Phys. Techn.* **2008**, *51*, 546.
[21] M. H. Mogim, M. H. Paydar, *Infrared Phys. Techn.* **2010**, *53*, 430.
[22] N. Bazin, J. E. Andrew, H. A. McInnes, *J. Sol-Gel Sci. Technol.* **1998**, *13*, 757.
[23] N. D. Zverev, E. M. Grasanov, K. G. Chan, M. B. Khotamov, *Soc. J. Optic. Technol.* **1991**, *58*, 361.
[24] A. Gombert, W. Glaubitt, K. Rose, J. Dreibhloz, B. Blasi, A. Heinzel, D. Sporn, W. Doll, V. Wittwer, *Thin Solid Films* **1999**, *351*, 73.
[25] S. Fujihara, M. Tada, T. Kimura, *Thin Solid Films* **1997**, *304*, 252.
[26] M. Tada, S. Fujihara, T. Kumura, *J. Mater. Res.* **1999**, *14*, 1610.
[27] A. A. Rywak, J. M. Burlitch, *Chem. Mater.* **1996**, *8*, 60.
[28] H. Krüger, E. Kemnitz, A. Hertwig, U. Beck, *Thin Solid Films* **2008**, *516*, 4175.
[29] H. Krüger, A. Hertwig, U. Beck, E. Kemnitz, *Thin Solid Films* **2010**, *518*, 6080.
[30] D. Grosso, C. Boissière, C. Sanchez, *Nature* **2007**, *6*, 572.
[31] J. D. Bass, C. Boissiere, L. Nicole, D. Grosso, C. Sanchez, *Chem. Mater.* **2008**, *20*, 5550.
[32] S. Fujihara, K. Tokumo, *J. Fluorine Chem.* **2009**, *130*, 1106.
[33] S. V. Kuznetsov, V. V. Osiko, E. A. Tkatchenko, P. P. Fedorov, *Russ. Chem. Rev.* **2006**, *75*, 1065.
[34] A. Saberi, Z. Negahdari, S. Bouazza, M. W. Porada, *J. Fluorine Chem.* **2010**, *131*, 1353.
[35] T. Skapin, G. Tavcar, A. Bencan, Z. Mazej, *J. Fluorine Chem.* **2009**, *130*, 1086.
[36] M. Caok, Y. Wang, Y. Qi, C. Guo, C. Hu, *J. Solid State Chem.* **2004**, *177*, 2205.
[37] M. Pietrowski, M. Wojciechowska, *J. Fluorine Chem.* **2007**, *128*, 219.
[38] I. Sevonkaev, E. Matijevic, *Langmuir* **2009**, *25*, 10534.
[39] I. Sevonkaev, D. V. Goia, E. Matijevic, *J. Colloid Interf. Sci.* **2008**, *317*, 130.
[40] A. B. D. Nandiyanto, F. Iskandar, T. Ogi, K. Okuyama, *Langmuir* **2010**, *26*, 12260.
[41] M. Wojciechowska, R. Fiedorow, *J. Fluorine Chem.* **1980**, *15*, 443.
[42] M. Wojciechowska, M. Zielinski, M. Pietrowski, *J. Fluorine Chem.* **2003**, *120*, 1.
[43] M. Wojciechowska, M. Pietrowski, M. Zielinski, *Catal. Today* **2007**, *119*, 338.
[44] M. Wojciechowska, M. Zielinski, M. Przystajko, M. Pietrowski, *Catal. Today* **2007**, *119*, 44.
[45] M. Pietrowski, M. Zielinski, M. Wojciechowska, *Catal. Lett.* **2009**, *128*, 31.
[46] V. N. Kalevaru, B. D. Raju, V. V. Rao, A. Martin, *Catal. Commun.* **2008**, *9*, 715.
[47] V. N. Kalevaru, B. D. Raju, V. V. Rao, A. Martin, *Appl. Catal. A* **2009**, *352*, 223.
[48] S. Wuttke, G. Scholz, S. Rüdiger, E. Kemnitz, *J. Mater. Chem.* **2007**, *17*, 4980.
[49] A. Dimitrov, S. Wuttke, S. Troyanov, E. Kemnitz, *Angew. Chem. Int. Ed.* **2008**, *47*, 190.
[50] S. Wuttke, A. Lehmann, G. Scholz, M. Feist, A. Dimitrov, S. I. Troyanov, E. Kemnitz, *Dalton Trans.* **2009**, 4729.
[51] J. K. Murthy, U. Groß, S. Rüdiger, E. Kemnitz, J. M. Winfield, *J. Solid State Chem.* **2006**, *179*, 739.
[52] S. Wuttke, A. Vimont, J.-C. Lavalley, M. Daturi, E. Kemnitz, *J. Phys. Chem. C* **2010**, *114*, 5113.
[53] A. Vimont, F. Thibault-Starzyk, M. Daturi, *Chem. Soc. Rev.* **2010**, *39*, 4928.
[54] G. Spoto, E. N. Gribov, G. Ricchiardi, A. Damin, D. Scarano, S. Bordiga, C. Lamberti, A. Zecchina, *Prog. Surf. Sci.* **2004**, *76*, 71.
[55] M. S. Nozari, R. S. Drago, *J. Am. Chem. Soc.* **1970**, *92*, 7086.
[56] E. Bosch, S. Huber, J. Weitkamp, *Phys. Chem. Chem. Phys.* **1999**, *1*, 579.
[57] S. Huber, H. Knözinger, *J. Mol. Catal. A* **1999**, *141*, 117.
[58] M. N. Amiry, G. Eltanany, S. Wuttke, S. Rüdiger, E. Kemnitz, J. M. Winfield, *J. Fluorine Chem.* **2008**, *129*, 366.
[59] K. Tanabe, *Bull. Chem. Soc. Jpn.* **1974**, *47*, 1064.
[60] E. Kemnitz, Y. Zhu, B. Adamczyk, *J. Fluorine Chem.* **2002**, *114*, 163.
[61] J. K. Murthy, U. Groß, S. Rüdiger, E. Ünveren, E. Kemnitz, *J. Fluorine Chem.* **2004**, *125*, 937.
[62] J. K. Murthy, U. Groß, S. Rüdiger, E. Kemnitz, *Appl. Catal. A* **2004**, *278*, 133.
[63] J. K. Murthy, U. Groß, S. Rüdiger, E. Ünveren, W. Unger, E. Kemnitz, *Appl. Catal. A* **2005**, *282*, 85.
[64] H. A. Prescott, Z.-J. Li, E. Kemnitz, J. Deutsch, H. Lieske, *J. Mater. Chem.* **2005**, *15*, 4616.
[65] S. Wuttke, S. M. Coma, J. Kröhnert, F. C. Jentoft, E. Kemnitz, *Catal. Today* **2010**, *152*, 2.
[66] S. Wuttke, S. M. Coman, G. Scholz, H. Kirmse, A. Vimont, M. Daturi, S. L. M. Schroeder, E. Kemnitz, *Chem. Eur. J.* **2008**, *14*, 11488.
[67] H. Knözinger, P. Ratnasamy, *Catal. Rev. Sci. Eng.* **1978**, *17*, 31.
[68] A. Negoi, S. Wuttke, E. Kemnitz, D. Macovei, V. I. Parvulescu, C. M. Teodorescu, S. M. Coman, *Angew. Chem. Int. Ed.* **2010**, *49*, 8134.
[69] F. W. Lytle, P. S. P. Wei, R. B. Greegor, G. H. Via, J. H. Sinfelt, *J. Chem. Phys.* **1979**, *70*, 4849.
[70] B. Hammer, J. K. Nørskov, *Nature* **1995**, *376*, 238.
[71] P. T. Patil, A. Dimitrov, H. Kirmse, W. Neumann, E. Kemnitz, *Appl. Catal. B* **2007**, *78*, 80.
[72] P. T. Patil, A. Dimitrov, J. Radnik, E. Kemnitz, *J. Mater. Chem.* **2008**, *18*, 1632.
[73] J. K. Murthy, U. Groß, S. Rüdiger, V. V. Rao, V. V. Kumar, A. Wander, C. L. Bailey, N. M. Harrison, E. Kemnitz, *J. Phys. Chem. B* **2006**, *110*, 8314.
[74] T. Krahl, A. Vimont, G. Eltanany, M. Daturi, E. Kemnitz, *J. Phys. Chem. C* **2007**, *111*, 18317.
[75] S. M. Coman, P. Patil, S. Wuttke, E. Kemnitz, *Chem. Commun.* **2009**, 460.
[76] S. M. Coman, V. I. Parvulescu, S. Wuttke, E. Kemnitz, *ChemCatChem* **2010**, *2*, 92.
[77] N. Candu, S. Wuttke, E. Kemnitz, S. M. Coman, V. I. Parvulescu, *Appl. Catal. A* **2011**, *391*, 169.
[78] K. Scheurell, G. Scholz, E. Kemnitz, *Solid State Sci.* **2007**, *180*, 749.
[79] K. Scheurell, G. Scholz, A. Pawlik, E. Kemnitz, *Solid State Sci.* **2008**, *10*, 873.
[80] S. Rüdiger, U. Gross, M. Feist, H. A. Prescott, S. C. Shekar, S. I. Troyanov, E. Kemnitz, *J. Mater. Chem.* **2005**, *15*, 588.
[81] Y. Zhu, K. Fiedler, S. Rüdiger, E. Kemnitz, *J. Catal.* **2003**, *219*, 8.
[82] E. Kemnitz, J. M. Winfield in *Advanced Inorganic Fluorides: Synthesis Characterization and Applications* (Eds.: T. Nakajima, A. Tressaud, B. Zemva), Elsevier, London, **2000**, p. 367.
[83] B. Adamczyk, O. Boese, N. Weiher, S. L. M. Schroeder, E. Kemnitz, *J. Fluorine Chem.* **2000**, *101*, 239.
[84] J. Thomson, G. Webb, J. M. Winfield, D. Bonniface, C. Shortman, N. Winterton, *Appl. Catal. A* **1993**, *97*, 67.
[85] A. Bendada, D. W. Bonniface, F. McMonagle, R. Marshall, C. Shortman, R. R. Spence, J. Thomson, G. Webb, J. M. Winfield, N. Winterton, *Chem. Commun.* **1996**, 1947.

[86] W. Bonrath, M. Eggersdorfer, T. Netscher, *Catal. Today* **2007**, *121*, 45.
[87] J. M. Tucker, D. M. Townsend, *Biomedicine Pharmacotherapy* **2005**, *59*, 380.
[88] K. Saldeen, T. Saldeen, *Nutrition Res.* **2005**, *25*, 877.
[89] W. Bonrath, M. Eggersdorfer, T. Netscher, *Catal. Today* **2007**, *121*, 45.
[90] W. Bonrath, T. Netscher, *Appl. Catal. A* **2005**, *280*, 55.
[91] M. Schneider, K. Zimmermann, F. Aquino, W. Bonrath, *Appl. Catal. A* **2001**, *220*, 51.
[92] Y. Kokubo, A. Hasegawa, S. Kuwata, K. Ishihara, H. Yamamoto, T. Ikariya, *Adv. Synth. Catal.* **2005**, *347*, 220.
[93] H. Wang, B.-Q. Xu, *Appl. Catal. A* **2004**, *275*, 247.
[94] M. C. Laufer, W. Bonrath, W. F. Hölderich, *Catal. Lett.* **2005**, *100*, 101.
[95] A. Heidekum, M. A. Harmer, W. F. Hölderich, *J. Catal.* **1998**, *176*, 260.
[96] S. Wang, F. Kienzle, *Ind. Eng. Chem. Res.* **2000**, *39*, 4487.
[97] A. Hasegawa, K. Ishihara, H. Yamamoto, *Angew. Chem. Int. Ed.* **2003**, *42*, 5731.
[98] F. M. D. Ismail, M. J. Hilton, M. Stefinovic, *Tetrahedron Lett.* **1992**, *33*, 3795.
[99] U. Svanholm, V. D. Parker, *J. Chem. Soc. Perkin Trans. 2* **1974**, *2*, 169.
[100] S. M. Coman, S. Wuttke, A. Vimont, M. Daturi, E. Kemnitz, *Adv. Synth. Catal.* **2008**, *350*, 2517.
[101] S. Wang, W. Bonrath, H. Pauling, F. Kienzle, *J. Supercritical Fluids* **2000**, *17*, 135 and references herein .
[102] K. Ishihara, M. Kubota, H. Yamamoto, *Synlett* **1996**, 1045.
[103] A. Rüttimann, *Chimia* **1986**, *40*, 290.
[104] H. Mayer, O. Isler in *The Vitamins*, *2nd Ed., Vol. III* (Eds.: W. H. Sebrell Jr., R. S. Harris), Academic Press, New York **1971**.
[105] K. Mukai, K. Okabe, H. Hosose, *J. Org. Chem.* **1989**, *54*, 557.
[106] T. W. Bastock, J. H. Clark, *Speciality Chemicals*, Elsevier, London, **1991**.
[107] B. M. Khadilkar, S. D. Borkar, *Chem. Technol. Biotechnol.* **1998**, *71*, 209.
[108] D. Yin, C. Li, L. Tao, N. Yu, S. Hu, D. Yin, *J. Mol. Catal. A* **2006**, *245*, 260.
[109] G. A. Olah, *Friedel–Crafts Chemistry*, Wiley, New York, **1973**.
[110] X. Hu, G. K. Chuah, S. Jaenicke, *Appl. Catal. A* **2001**, *217*, 1.
[111] S. Sebti, R. Tahir, R. Nazih, S. Boulaajaj, *Appl. Catal. A* **2001**, *218*, 25.
[112] F. Neatu, S. Coman, V. I. Parvulescu, G. Poncelet, D. de Vos, P. A. Jacobs, *Top. Catal.* **2009**, *52*, 1292.
[113] A. Comas-Vives, C. Gonzalez-Arellano, A. Corma, M. Iglesias, F. Sanchez, G. Ujaque, *J. Am. Chem. Soc.* **2006**, *128*, 4756.

Received: May 26, 2011
Published Online: October 10, 2011

